



HANAN CHWEIH

ESPECIFICIDADES TECIDUAIS E DE SEXO NO
TRANSPORTE DE Ca^{2+} POR MITOCÔNDRIAS ISOLADAS:
AVALIAÇÕES EM CONDIÇÕES QUE IMPEDEM A
TRANSIÇÃO DE PERMEABILIDADE

*TISSUE AND SEX SPECIFICITIES IN THE Ca^{2+} HANDLING
BY ISOLATED MITOCHONDRIA: EVALUATIONS UNDER
CONDITIONS AVOIDING THE PERMEABILITY TRANSITION*

CAMPINAS
2015



UNIVERSIDADE ESTADUAL DE CAMPINAS
Faculdade de Ciências Médicas

HANAN CHWEIH

ESPECIFICIDADES TECIDUAIS E DE SEXO NO TRANSPORTE DE Ca^{2+}
POR MITOCÔNDRIAS ISOLADAS: AVALIAÇÕES EM CONDIÇÕES QUE
IMPEDEM A TRANSIÇÃO DE PERMEABILIDADE

*TISSUE AND SEX SPECIFICITIES IN THE Ca^{2+} HANDLING BY ISOLATED
MITOCHONDRIA: EVALUATIONS UNDER CONDITIONS AVOIDING THE
PERMEABILITY TRANSITION*

Dissertação de Mestrado apresentada à Pós-Graduação da Faculdade de Ciências Médicas da Universidade Estadual de Campinas – UNICAMP para obtenção de título de Mestra em Ciências.

Master's thesis submitted to the Graduate School of Medical Sciences, State University of Campinas - UNICAMP to obtain the Master Degree in Sciences.

ORIENTADOR: Prof. Dr. TIAGO REZENDE FIGUEIRA
CO-ORIENTADOR: Prof Dr. ROGER FRIGÉRIO CASTILHO

ESTE EXEMPLAR CORRESPONDE À VERSÃO
FINAL DA DISSERTAÇÃO DEFENDIDA POR
HANAN CHWEIH, ORIENTADA PELO PROF.
DR. TIAGO REZENDE FIGUEIRA.

Assinatura do Orientador

CAMPINAS
2015

Ficha catalográfica
Universidade Estadual de Campinas
Biblioteca da Faculdade de Ciências Médicas
Maristella Soares dos Santos - CRB 8/8402

C478e Chweih, Hanan, 1990-
Especificidades teciduais e de sexo no transporte de
Ca²⁺ por mitocôndrias isoladas : avaliações que
impedem a transição de permeabilidade / Hanan Chweih.
-- Campinas, SP : [s.n.], 2015.

Orientador : Tiago Rezende Figueira.
Coorientador : Roger Frigério Castilho.
Dissertação (Mestrado) - Universidade Estadual de
Campinas, Faculdade de Ciências Médicas.

1. Uniporter mitocondrial de calcio. 2. Transição de
permeabilidade mitocondrial. 3. Homeostase. 4. Troca
iônica. I. Figueira, Tiago Rezende, 1980-. II. Castilho,
Roger Frigério, 1972-. III. Universidade Estadual de
Campinas. Faculdade de Ciências Médicas. IV. Título.

Informações para Biblioteca Digital

Título em outro idioma: Tissue and sex especificities in the Ca²⁺ handling by isolated
mitochondria : evaluations under conditions avoiding the permeability transition

Palavras-chave em inglês:

Mitochondrial calcium uniporter
Mitochondrial permeability transition
Homeostasis
Ion exchange

Área de concentração: Fisiopatologia Médica

Titulação: Mestra em Ciências

Banca examinadora:

Tiago Rezende Figueira [Orientador]
Luciane Carla Alberice
Rosana Almada Bassani

Data de defesa: 27-03-2015

Programa de Pós-Graduação: Fisiopatologia Médica

BANCA EXAMINADORA DA DEFESA DE MESTRADO

HANAN CHWEIH

Orientador (a) PROF(A). DR(A). TIAGO REZENDE FIGUEIRA

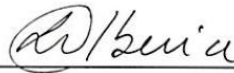
Coorientador (a) PROF(A). DR(A). ROGER FRIGERIO CASTILHO

MEMBROS:

1. PROF(A). DR(A). TIAGO REZENDE FIGUEIRA



2. PROF(A). DR(A). LUCIANE CARLA ALBERICE



3. PROF(A). DR(A). ROSANA ALMADA BASSANI



Programa de Pós-Graduação em Fisiopatologia Médica da Faculdade de Ciências Médicas da Universidade Estadual de Campinas

Data: 27 de março de 2015

RESUMO

Algumas das características das mitocôndrias, incluindo as suas funções de transporte de Ca^{2+} , podem apresentar dimorfismo sexual e especificidades teciduais. No entanto, as mensurações do transporte de Ca^{2+} em mitocôndrias isoladas estão sujeitas a artefatos secundários a abertura do poro de transição de permeabilidade mitocondrial (PTP) induzido pelo acúmulo excessivo de Ca^{2+} nesta organela. Neste estudo, o objetivo inicial foi avaliar se a inibição do PTP pela ciclosporina A (CsA) afeta a mensuração de diversas variáveis que descrevem o transporte de Ca^{2+} por mitocôndrias isoladas de fígado de rato. Os resultados obtidos indicam que as concentrações de estado estável do Ca^{2+} externo a mitocôndria e as taxas de efluxo mitocondrial de Ca^{2+} através de trocadores seletivos foram superestimados em até 4 vezes quando o PTP não foi inibido farmacologicamente pela CsA. O objetivo subsequente foi analisar o transporte de Ca^{2+} em mitocôndrias isoladas de fígado, de músculo esquelético, de coração e de cérebro de ratos machos e fêmeas sob condições experimentais específicas (i.e. meio de incubação contendo inibidores TPM, substratos energéticos ligados a NAD e níveis relevantes de Ca^{2+} , Mg^{2+} e Na^+). Os dados indicaram que a taxa de influxo de Ca^{2+} em mitocôndrias de fígado foi ~4 vezes superior à dos outros tecidos, as quais foram semelhantes entre si. Em contrapartida, as taxas de efluxo de Ca^{2+} apresentaram uma maior diversidade entre tecidos, especialmente na presença de Na^+ . Curiosamente, o efluxo de Ca^{2+} na ausência de Na^+ foi significativamente mais elevado nas mitocôndrias cardíacas (~4nmol/mg/min) em relação às taxas observadas nos outros tecidos, contrariando a concepção de que o efluxo de Ca^{2+} de mitocôndrias de coração é dependente, quase que exclusivamente, de um trocador que requer Na^+ . A especificidade em relação ao sexo só foi observada em dois índices relacionados à homeostase mitocondrial de Ca^{2+} (i.e. cinética geral normalizada da captação de Ca^{2+} e a concentração de estado estável do Ca^{2+} externo a mitocôndria) em mitocôndrias isoladas de coração (mais lentos ou maiores na fêmea) e na respiração estimulada por ADP em mitocôndrias de fígado (~20% maior na fêmea). O presente estudo demonstrou a importância metodológica de se prevenir a abertura do PTP para a análise das propriedades e da variabilidade fisiológica do transporte de Ca^{2+} por mitocôndrias isoladas. Adicionalmente, concluímos que sob as condições experimentais aqui utilizadas, o efluxo de Ca^{2+} mitocondrial apresenta grandes especificidades teciduais e que alguns achados desafiam conceitos estabelecidos em estudos anteriores sob condições arguivelmente menos controladas.

Palavras-chave: Mitochondrial Calcium Uniporter (MCU), transporte mitocondrial de Ca^{2+} , transição de permeabilidade mitocondrial, homeostase de Ca^{2+} , troca iônica mitocondrial.

ABSTRACT

The characteristics of mitochondria, including their Ca^{2+} transport functions, may exhibit tissue specificity and sex dimorphism. Because the measurements of the Ca^{2+} handling by isolated mitochondria may be biased by dysfunction secondary to Ca^{2+} -induced mitochondrial permeability transition (MPT) pore opening, this study evaluates the extent to which MPT inhibition by cyclosporine-A affects the measurement of Ca^{2+} transport in isolated rat liver mitochondria. The results indicate that the steady-state levels of external Ca^{2+} and the rates of mitochondrial Ca^{2+} efflux through the selective pathways can be overestimated by up to 4-fold if MPT pore opening is not prevented. Then, we analyzed the Ca^{2+} transport in isolated mitochondria from the liver, skeletal muscle, heart and brain of male and female rats under incubation conditions containing MPT inhibitors, NAD-linked substrates and relevant levels of free Ca^{2+} , Mg^{2+} and Na^+ . Except for the liver mitochondria displaying values 4-fold higher, the Ca^{2+} influx rates were similar among the other tissues. In contrast, the Ca^{2+} efflux rates exhibited more tissue diversity, especially in the presence of Na^+ . Interestingly, the Na^+ -independent Ca^{2+} efflux was highest in the heart mitochondria (~ 4 nmol/mg/min), thus challenging the view that heart mitochondrial Ca^{2+} efflux relies almost exclusively on a Na^+ -dependent pathway. Sex specificity was only observed in two kinetic indexes (i.e. the normalized overall kinetics of Ca^{2+} uptake and the steady-state levels of external Ca^{2+}) of heart mitochondrial Ca^{2+} homeostasis (slower or higher in female) and in the ADP-stimulated respiration of liver mitochondria ($\sim 20\%$ higher in females). The present study shows the methodological importance of preventing MPT when measuring the properties and the physiological variability of the Ca^{2+} handling by isolated mitochondria. Moreover, we conclude that mitochondrial Ca^{2+} efflux exhibits great tissue specificity under our conditions, which may challenge some concepts raised in previous studies that employed experimental conditions that are arguably not well controlled.

Keywords: mitochondrial calcium uniporter, mitochondrial calcium transport, mitochondrial permeability transition, calcium homeostasis, mitochondrial ion exchange

SUMÁRIO

1. Introdução.....	01
1.1 Geração do potencial eletroquímico através da membrana mitocondrial interna.....	02
1.2 Transporte de Ca^{2+} por mitocôndrias.....	08
1.2.1 Influxo de Ca^{2+} por mitocôndrias.....	09
1.2.1.1. A identidade do MCU.....	10
1.2.2 O efluxo de Ca^{2+} por mitocôndrias.....	15
1.2.3 Transição de Permeabilidade Mitocondrial (TPM).....	17
2. Objetivos.....	20
3. * Capítulo: <i>Tissue and sex specificities in the Ca^{2+} handling by isolated mitochondria: Evaluations under conditions avoiding the permeability transition</i>	21
4. Conclusões.....	55
5. Referências.....	56
6. Anexo.....	62

*Esta dissertação é apresentada no formato alternativo de “artigo científico”. O artigo gerado por essa dissertação de mestrado é apresentada como um capítulo dela.

AGRADECIMENTOS

Agradeço a Deus por me amparar nos momentos difíceis, me dar força interior para superar as dificuldades, mostrar os caminhos nas horas incertas, me suprir em todas as necessidades e acima de tudo estar sempre no comando da minha vida.

Agradeço ao meu orientador Dr. Tiago Rezende Figueira por todos os ensinamentos durante esses dois anos, pela paciência em explicar e junto comigo buscar soluções, foi um grande responsável no meu processo principalmente de amadurecimento.

Agradeço ao meu co-orientador Prof. Dr. Roger Frigério Castilho por me conceder a oportunidade de desenvolver meu trabalho em seu laboratório, por estar sempre presente e disposto a discutir os resultados e sempre com alguma solução ou alternativa para nos auxiliar.

Agradeço ao meu pai Hermes Chweih que é meu exemplo de ser humano de garra e coragem, foi meu incentivador em todos os momentos esteve sempre ao meu lado não me deixando faltar nada, e acima de tudo se fez sempre presente mesmo quando a saudade falava mais alto.

A minha mãe Samira Zeinedin Chweih em quem eu me espelho sempre por ser a grande profissional que é por me mostrar que para nossos sonhos não existem limites e que nada na vida é impossível, esteve comigo sempre e jamais deixou que eu fraquejasse.

Agradeço a minha irmã Luana Chweih por ser a minha cúmplice, por cuidar de toda a minha família em minha ausência, por transformar as minhas noites em

alegrias com suas mensagens, e por cuidar do meu coração que sempre esteve com ela.

Agradeço ao meu namorado Felipe Vendrame que é a pessoa que esteve do meu lado em todos os momentos, sabe exatamente tudo que eu passei cada choro, cada alegria, me apoiou sempre e me fez perceber o quanto eu era capaz, jamais me deixou desistir, nem me deixou desamparada, foi meu porto seguro durante todo o tempo, sem você seria muito difícil eu te amo eternamente.

Agradeço a Audrey de Moraes, Ana Carolina Marques e Edilene dos Santos que são grandes amigas que eu fiz nesse tempo, estiveram sempre comigo e me trouxeram muitas alegrias, são amigas que já foram eternizadas.

Agradeço aos funcionários do laboratório pela disponibilidade sempre em ajudar Juliana Ronchi, Marcia Fagian e Roberto Stahl.

Agradeço aos técnicos do biotério pelo cuidado com meus animais, e prestatividade em todos os momentos que necessitei.

Agradeço aos colegas do Laboratório de Bioenergética: Erika Rodrigues, Genoefa Dal'óbó, Claudia Navarro, Estela Busanello, Felipe Ravagnani, Raffaella Ignarro, Gustavo Facchini, Juliana Ruas, Kezia Moura, Evellyne Figueiroa, Mary Aranda, Arthur Hernandez, Silva Mello, Franco Rossato, Rute Costa.

Agradeço, porém, com muitas saudades do meu grande amigo e confidente Paolo La Guardia (*in memoriam*) sua presença está fazendo muita falta neste momento.

Agradeço as agências de fomento Capes, Cnpq e FAPESP por financiar e acreditar no projeto.

LISTA DE FIGURAS

Figura 1- Fosforilação Oxidativa.....	05
Figura 2- Imagem 3D por tomografia eletrônica de mitocôndria de fígado de rato.....	07
Figura 3- Representação do complexo proteico MCU.....	12
Figura 4-Representação esquemática das estruturas proteicas envolvidas no transporte mitocondrial de Ca^{2+}	17

LISTA DE ABREVIATURAS

$\Delta\psi$ Potencial elétrico de membrana

ADP Difosfato de Adenosina

ATP Trifosfato de Adenosina

Ca²⁺ Íons de Cálcio

CsA Ciclosporina A

CypD Ciclofilina D

DNA Ácido desoxirribonucléico

EMRE *Essential MCU Regulator*

EROs Espécies reativas de oxigênio

FADH₂ Dinucleotídeo de flavina-adenina reduzido

MCU *Mitochondrial calcium uniporter*

MCUR *Mitochondrial calcium uniporter regulator*

MICU1 *Mitochondrial calcium uptake 1*

MICU2 *Mitochondrial calcium uptake 2*

MME Membrana mitocondrial externa

MMI Membrana mitocondrial interna

NAD⁺ Dinucleotídeo de nicotinamida- adenina – forma oxidada

NADH Dinucleotídeo de nicotinamida- adenina – forma reduzida

NADP⁺ Dinucleotídeo de nicotinamida- adenina- fosfato, forma oxidada

R.R Ruthenium Red (Vermelho de Rutênio)

ANT Translocador de nucleotídeo de adenina

TPM Transição de permeabilidade mitocondrial

UCP Proteína desacopladora

VDAC Canal aniônico dependente de voltagem

1.INTRODUÇÃO

As primeiras descobertas sobre a existência das mitocôndrias como organelas foram realizadas por Rudolph Albert Von Kölliker em 1857; ele as classificou como compartimentos citoplasmáticos granulares presentes nos músculos, e as denominou sarcossomos de Kölliker. Em seguida surgiram outras denominações diferentes para a mesma organela, entre os quais se destaca o trabalho realizado por Benda (1898) *Apud* [1] que se referiu a esta organela como “*mitochondrion*”, do grego mito (filamento) e chondron (grão). Considerando que esta denominação parece ser a que melhor representava as características morfológicas dessa organela, essa terminologia passou a ser utilizada desde meados da década de 1930 [1].

Hogeboom, Schneider e Palade em (1948) *Apud* [1] conseguiram pela primeira vez isolar mitocôndrias intactas de fígado de rato por meio do método de centrifugação diferencial e em 1950 Palade e Sjöstrand publicaram imagens de microscopia eletrônica de alta resolução de mitocôndrias, nas quais era possível observar suas características ultraestruturais. Na segunda metade da década de 40, os bioquímicos Eugene Kennedy e Albert Lehninger demonstraram que a mitocôndria era a organela majoritariamente responsável pela síntese do ATP na célula, e que isto acontecia de forma associada à oxidação de coenzimas reduzidas (NADH⁺ e FADH₂). Na sequência, vários estudos foram realizados visando à compreensão do mecanismo responsável pelo acoplamento termodinâmico entre a respiração mitocondrial e a síntese de ATP [1-3].

Na década de 60, estabeleceu-se o conceito de organela independente (não muito correto à luz de hoje) com a descoberta do DNA mitocondrial. Posteriormente o DNA mitocondrial constitui-se um dos indícios que reforçariam a hipótese da origem endossimbiótica das mitocôndrias, como proposto por Altmann já em 1890 [4]. Neste período

da história sobre mitocôndria, o bioquímico Peter Mitchell propôs a teoria quimiosmótica da fosforilação oxidativa em 1961, baseada na constatação de que cadeia respiratória promove a redução do O_2 à H_2O , enquanto gera um gradiente de prótons (H^+) através da membrana mitocondrial interna (MMI); em sua teoria, a energia estocada na forma de gradiente eletroquímico seria utilizada para promover a reação da fosforilação do ADP em ATP [5].

Muito se avançou e o conceito atual é de que as mitocôndrias são as organelas intracelulares responsáveis pela conversão de energia de óxido-redução (potencial de oxidação-redução) contida nos nutrientes energéticos em energia química na forma de ATP. De maneira geral, esta conversão de energia ocorre à medida que elétrons são transferidos dos substratos energéticos, por intermédio de coenzimas carreadoras de elétrons, para o oxigênio; este processo é denominado respiração celular e representa o mecanismo principal de transdução de energia útil (i.e. disponível para realizar trabalho) em seres aeróbios [1]. Além desta função na transdução de energia, as mitocôndrias podem ser uma das principais fontes geradoras de espécies reativas de oxigênio (EROs) nas células [6]. O papel da mitocôndria como um sítio de compartimentalização do Ca^{2+} celular será discutido detalhadamente a seguir.

1.1 Geração do potencial eletroquímico através da membrana mitocondrial interna

A mitocôndria é constituída por duas membranas, a interna e a externa. A membrana mitocondrial externa (MME) tem alta permeabilidade em relação àquela da membrana interna; esta permeabilidade é conferida principalmente pela proteína integral porina, também conhecida como canal aniônico voltagem dependente (VDAC- voltage dependent anion channel) [7].

A MMI é impermeável à maioria das moléculas e a íons, incluindo o H^+ ; porém é permeável ao O_2 , CO_2 , $NO\bullet$, H_2O e H_2O_2 . Diversas espécies químicas atravessam a membrana interna através de transportadores específicos, como por exemplo: ATP^{-4} e ADP^{-3} , transportado pelo ANT (translocador de nucleotídeo de adenina); piruvato, transportado pelo PiC (*pyruvate carrier*), entre vários outros. Na membrana interna se encontram os complexos proteicos multissubunidades denominados complexos respiratórios; o conjunto dos 4 complexos respiratórios montados na MMI é conhecido como cadeia transportadora de elétrons. Há ainda a ATP-sintase, algumas vezes descrita (erroneamente) como complexo V da cadeia transportadora de elétrons. A integração (acoplamento termodinâmico) entre a cadeia transportadora de elétrons e a atividade da ATP-sintase é responsável pelo processo de fosforilação oxidativa do ADP em ATP [6, 8].

Os elétrons procedentes das coenzimas NADH e $FADH_2$, reduzidas durante o metabolismo oxidativo de substratos energéticos são transferidos ao complexo I (NADH desidrogenase) e ao complexo II (succinato desidrogenase) respectivamente. O complexo I transfere seus elétrons à forma oxidada da coenzima Q (Q), gerando a forma reduzida desta coenzima (QH_2) [2]. Elétrons originados a partir do succinato passam para a Q através do complexo II. Em alguns tecidos, a coenzima Q pode também ser reduzida pela glicerol-3-fosfato desidrogenase (um complexo enzimático com seu sítio catalítico voltado para a face externa da MMI) que transfere os elétrons doados pelo glicerol-3-fosfato citosólico. A coenzima Q também pode ser reduzida a QH_2 pela ação da FTP: ubiquinona oxirredutase, a qual está montada na face interna da membrana mitocondrial interna. Esta enzima recebe elétrons doados pela proteína FTP que é reduzida na primeira etapa da β -oxidação de ácidos graxos. A QH_2 é então oxidada pelo complexo III, resultando na formação de uma coenzima Q parcialmente reduzida (radical aniônico semiquinona- $QH\bullet$); para completar o ciclo que transfere 2 elétrons da QH_2 para dois citocromos C, uma segunda QH_2 deve ser oxidada

pelo complexo III, de forma que o radical semiquinona ($\text{QH}\cdot$) será reduzido monoelétricamente para se transformar em coenzima Q totalmente reduzida (i.e. QH_2) – esta transferência em duas etapas dos elétrons da QH_2 para o citocromo C por intermédio do complexo III é conhecida como ciclo Q. O citocromo C transfere elétrons para uma das subunidades transportadoras de elétron do complexo IV (também conhecido como citocromo C oxidase); o complexo IV é o responsável pela transferência dos elétrons entregues na cadeia respiratória para o seu acceptor final, o O_2 . Neste último passo da cadeia transportadora de elétrons o O_2 será então reduzido a H_2O [1, 7].

De acordo com a teoria quimiosmótica de *Mitchell 1961* [5], com a passagem de elétrons através da sequência de intermediários redox da cadeia respiratória, ocorre ejeção de H^+ da matriz mitocondrial para o espaço intermembrana, gerado um gradiente de H^+ (gradiente eletroquímico) entre a matriz e o espaço intermembranas. De fato está ejeção de H^+ ocorre pela ação dos complexos I, III e IV, com as seguintes estequiometrias individuais: 4H^+ , 4H^+ e 2H^+ para cada par de elétrons transportado nos respectivos complexos respiratórios.

O gradiente formado pelo componente elétrico (~ 180 mV) e pelo componente químico (diferença de 0,75 unidade de pH) resultaria na formação de uma forma de energia que foi denominada de força próton-motriz. Esta forma de estocagem de energia é responsável pelo acoplamento termodinâmico entre a oxidação de substratos e a utilização desta energia para geração de ATP pela mitocôndria [5].

A ATP sintase é constituída de duas porções distintas, denominadas F_1 (protunde da MMI para a matriz mitocondrial) e F_0 (hidrofóbica e inserida na membrana mitocondrial interna). O fluxo de H^+ (a favor do gradiente) através das subunidades F_0 da ATP sintase de volta ao interior da mitocôndria provém à energia para a fosforilação do ADP em ATP pela porção F_1 [5]; a estequiometria intrínseca desta reação promovida ATP sintase é de 10H^+

transportados a favor do gradiente para a fosforilação de 3 ADP em 3 ATP. Esse processo geral da fosforilação oxidativa é demonstrado na figura 2.

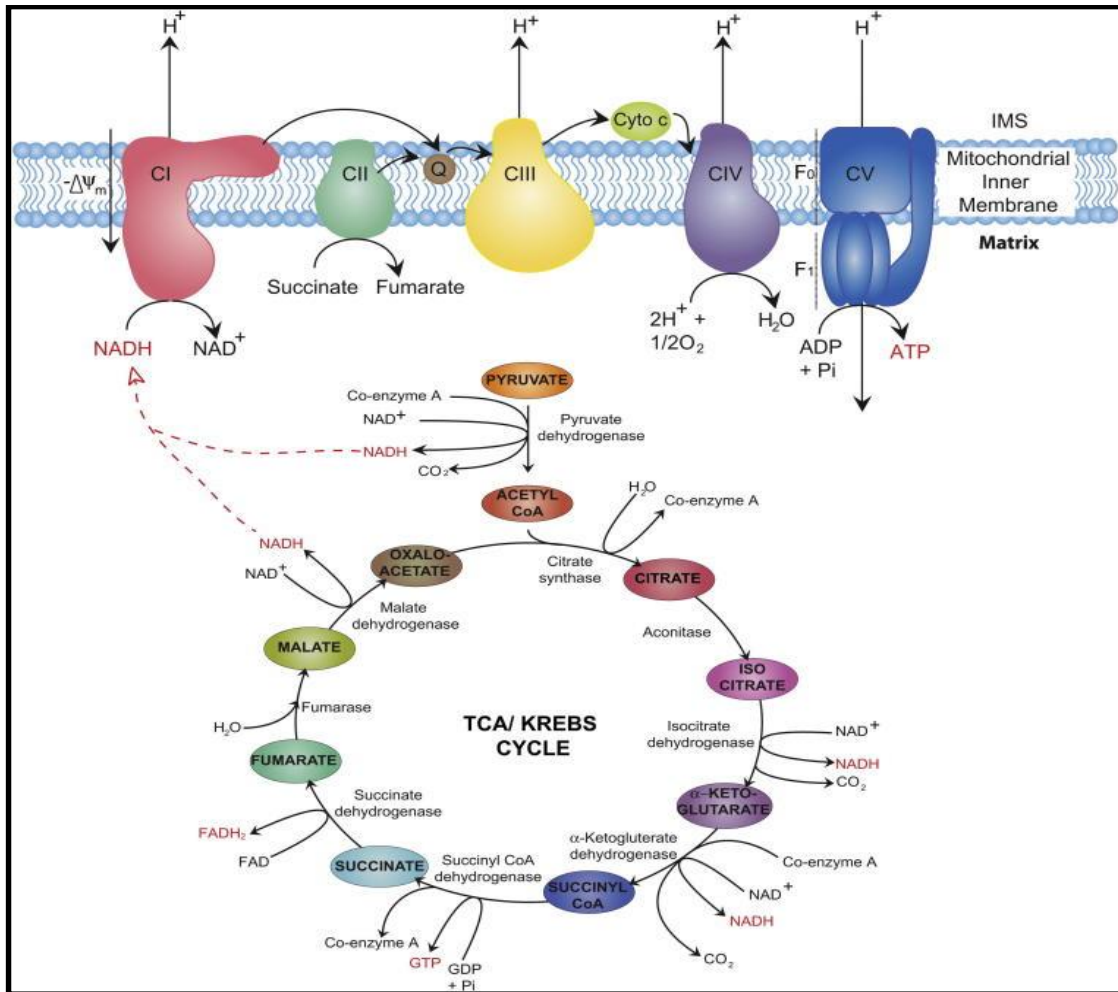


Figura 1. Fosforilação Oxidativa. Esquema ilustrativo da oxidação de piruvato pelo ciclo de Krebs e da fosforilação oxidativa (adaptado de Osellame et al 2012 [9]). A oxidação do piruvato através do ciclo de Krebs gera a redução de NAD^+ e FAD^+ . O NADH é por sua vez oxidado a NAD^+ pelo complexo I da cadeia transportadora de elétrons. A transferência de elétrons através desta cadeia, dos seus sítios de entrada até o oxigênio no complexo IV, gera um potencial eletroquímico transmembrana via bombeamento de H^+ da matriz mitocondrial para o espaço intermembrana. Este potencial eletroquímico é a forma de energia utilizada ATP sintase para fosforilar ADP em ATP.

É importante realçar que a força próton-matriz gerada pela respiração mitocondrial não serve apenas para a síntese de ATP pelas mitocôndrias. Ele também pode ser usado diretamente para promover processos endergônicos que não são energizados pela energia química do ATP. A seguir estão exemplos de processos endergônicos energizados pela

força próton-motriz: troca eletroforética de ATP^{4-} por ADP^{3-} , redução de NADP^+ pela transidrogenase específica, a captação eletroforética de Ca^{2+} , além do transporte de vários substratos [1, 5]. Ou seja, o transporte ativo através da membrana mitocondrial interna utiliza-se da energia armazenada como força próton-motriz.

Ainda na membrana interna encontram-se outras proteínas que atraem bastante interesse do ponto de vista da termodinâmica, como a proteína desacopladora (UCP). A UCP quando ativada permite o retorno de H^+ ao interior da matriz mitocondrial, causando dissipação parcial do potencial eletroquímico transmembrana e, então, desacoplamento entre respiração (oxidação dos nutrientes e transferência de elétrons ao oxigênio) e fosforilação do ADP em ATP. Esse processo gera um ciclo fútil de H^+ através da membrana mitocondrial interna, promovendo a dissipação da energia do potencial eletroquímico sob a forma de calor [10], uma forma de energia inútil em sistemas biológicos. Em animais há predomínio da UCP1 no tecido adiposo marrom, órgão especializado em produzir calor e contribuir para a homeotermia. Há outras isoformas de UCPs (UCP2 e 3) expressas em outros tecidos de mamíferos, porém suas funções desacopladoras não são totalmente estabelecidas. As funções destas outras isoformas de UCP parecem ser relacionadas a um mecanismo de controle da produção das EROs mitocondriais ou defesa antioxidante [11].

O compartimento demarcado pela membrana mitocondrial interna é designado matriz mitocondrial, cujo volume pode variar dependendo do estado funcional da mitocôndria [12, 13]. A matriz contém ribossomos, DNA mitocondrial e várias enzimas; estas enzimas são especialmente conhecidas e importantes para o metabolismo energético, pois catalisam o ciclo de Krebs (degradação do acetil-coA e redução das coenzimas NAD e FAD), a β -oxidação (degradação dos ácidos graxos), a oxidação de aminoácidos e a oxidação do piruvato a Acetil-CoA [1, 14, 15].

O compartimento delimitado entre as duas membranas descritas acima é designado espaço intermembranas. Ele contém cerca de 50 diferentes proteínas envolvidas em diversas funções, como: fatores que desencadeiam apoptose quando liberados para o citosol, transportadores de metabólitos, proteases, enzimas e um amplo número de fatores responsáveis pela formação dos arranjos dos complexos da cadeia respiratória, além de íons, metais e lipídios [16].

A morfologia destas duas membranas e dos compartimentos descritos acima foi bastante clarificada pelo estudo de Mannella *et al* [17] (Figura 2). Estes autores obtiveram imagens elaboradas que revelaram a organização espacial da ATP sintase e dos complexos da cadeia transportadora de elétrons na MMI, demonstrando que as invaginações das cristas da membrana mitocondrial interna são pleomórficas, ligadas por meio de estreitos segmentos tubulares de comprimento variável.

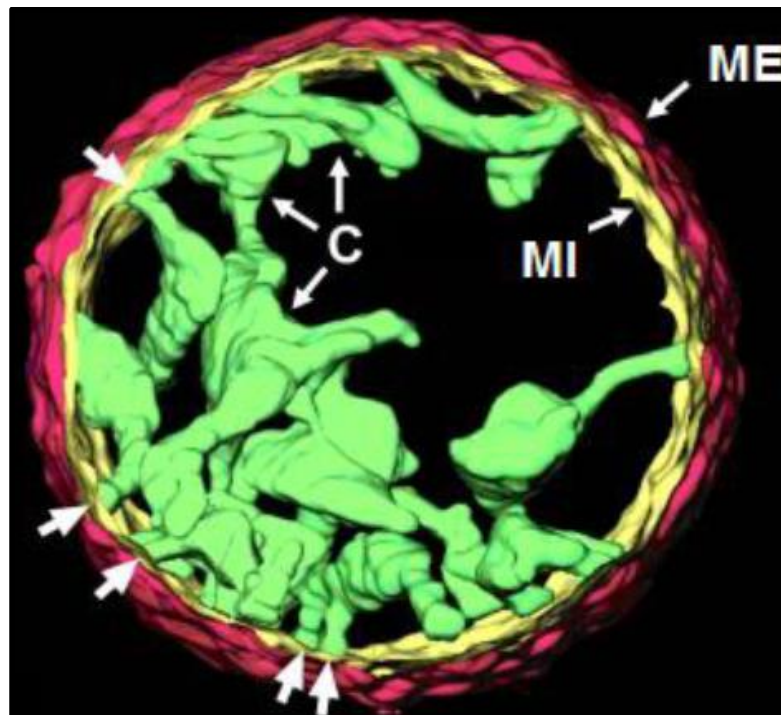


Figura 2. Imagem 3D de mitocôndria de fígado de rato. Imagem reconstruída a partir de tomografia eletrônica de mitocôndria isolada de fígado de rato. Membrana externa (ME), membrana interna (MI) e cristas (C). As setas não nomeadas apontam para regiões de ligações tubulares estreitas da crista MME Adaptado de Mannella 2001 [17].

1.2 Transporte de Ca^{2+} por mitocôndrias

Sistemas biológicos possuem transportadores de Ca^{2+} e de outros íons que coordenamos fluxos de íons específicos através das membranas celulares em resposta a sinais celulares e extracelulares [18]. O Ca^{2+} é o principal íon com função sinalizadora em sistemas biológicos.

No início do desenvolvimento do conhecimento sobre as funções e características das mitocôndrias, estas organelas já foram associadas à movimentação de Ca^{2+} através de sua membrana interna, a qual possui permeabilidade altamente seletiva. Assim, há mais de 50 anos já se acreditava que as mitocôndrias eram capazes de sequestrar Ca^{2+} através de um mecanismo ativo (uma vez que o Ca^{2+} é sequestrado contra um gradiente de concentração) [19, 20], fazendo uso direto da energia retirada da oxidação dos substratos. Essa ideia se tornou mais robusta quando se verificou que as mitocôndrias renais de ratos eram capazes de captar grandes quantidades de Ca^{2+} [21, 22] e que este processo era acoplado à respiração [22]. Algumas propriedades importantes deste processo logo foram identificadas, tais como: captação de Ca^{2+} é inibida por inibidores da cadeia respiratória e desacopladores de fosforilação oxidativa [22]; não requer hidrólise de ATP como mecanismo primário de transferência de energia [23].

No entanto para o Ca^{2+} acumular-se na matriz mitocondrial ele deve atravessar as duas membranas mitocondriais, a externa e a interna. A MME é permeável a solutos ≤ 5 kDa, e portanto também ao Ca^{2+} ; essa alta permeabilidade da MME é principalmente devido à sua proteína mais abundante, o canal ânion dependente da voltagem (VDAC), que permite o "vaivém" de todos os metabólitos relacionados com o metabolismo energético, incluindo movimento de succinato, piruvato, malato, NADH, ATP, ADP e fosfato entre o citosol e o espaço intermembranas. Porém a atenção tem sido depositada principalmente sobre os

sistemas de transporte de íons da MMI, uma vez que ela tem permeabilidade altamente seletiva [24, 25].

A proteína responsável pelo transporte de Ca^{2+} através da MMI e os aspectos energéticos deste transporte foram objetos de intensa pesquisa científica por várias décadas e contínua até os dias atuais.

O transporte de Ca^{2+} pela mitocôndria de mamíferos ocorre através de mecanismos separados para intermediar influxo e efluxo. Estes dois fluxos opostos resultam movimento de Ca^{2+} através da membrana mitocondrial interna [26]. O balanço entre as taxas de influxo e de efluxo de Ca^{2+} compreende um determinante cinético de distribuição de Ca^{2+} entre o citosol e a matriz mitocondrial [27].

1.2.1 O Influxo de Ca^{2+} por mitocôndria

O influxo de Ca^{2+} para a mitocôndria é sensível alguns compostos, dentre eles *Ruthenium Red* (RR) e Ru360 são inibidores que foram utilizados amplamente nas pesquisas sobre transporte mitocondrial de Ca^{2+} . O Ru360 é um derivado mais purificado do RR, descrito pela primeira vez em 1991 [28]. A descoberta de inibidores da captação mitocondrial de Ca^{2+} foi fundamental para o avanço do conhecimento e ela se deu por Vinogradov *et al* [29]. Estes autores constataram que a captação de Ca^{2+} pela mitocôndria era inibida por lantanídeos - adições de RR em concentração μM baixa em ensaios de captação de Ca^{2+} por mitocôndrias promoviam o bloqueio do influxo de Ca^{2+} para a organela.

A relação entre as taxas de influxo de Ca^{2+} e a concentração de Ca^{2+} livre extramitocondrial foi historicamente bem explorada sob a perspectiva de cinéticas hiperbólicas ou sigmoidais, à semelhança da cinética de reações enzimáticas. Em função disto, valores de $V_{\text{máx}}$ e $K_{0,5}$ (análogo do K_m de enzimas *Michellianas*) foram determinados em mitocôndrias isoladas de vários tecidos. O influxo mitocondrial de Ca^{2+} descritos pelo

$V_{\text{máx}}$ e $K_{0,5}$ difere significativamente entre diferentes tecidos. Em mitocôndrias cardíacas foi demonstrada uma relação sigmoidal com $K_{0,5}$ variando de 10 a 15 μM ; no fígado há também uma relação sigmoidal e o $K_{0,5}$ varia de 24 a 27 μM . A $V_{\text{máx}}$ [30] da taxa de influxo de Ca^{2+} é geralmente maior no fígado (varia de 700 a 1200 nmol/mg/min) em relação ao coração (varia de 280 a 600 nmol/mg/min) [19]. No entanto, o valor mais alto de $V_{\text{máx}}$ relatado foi de 1750 nmol/mg/min, obtido em mitocôndrias cardíaca de cão preparadas com o método de digestão do tecido pela protease Nagase [31]. É de consenso geral há décadas que o $V_{\text{máx}}$ pode refletir uma barreira energética (sustentação do potencial eletroquímico transmembrana pelo sistema de transporte de elétrons) ao invés de um limite intrínseco da entidade molecular que intermedeia o influxo de Ca^{2+} para a mitocôndria [30].

Foi pouco difundida a ideia de que estas relações hiperbólicas ou sigmóides que levam a uma assíntota (isto é, $V_{\text{máx}}$) podem ser artefatos de disfunção mitocondrial associada às concentrações elevadas de Ca^{2+} . As concentrações de Ca^{2+} necessárias para se observar uma assíntota em estudos cinéticos são também concentrações que promovem dano a estrutura e função da organela; logo, a observação de uma assíntota (estimativa do $V_{\text{máx}}$) pode redundar de disfunção induzida por Ca^{2+} e ter nenhum significado do ponto de vista cinético e biológico do processo de influxo de Ca^{2+} para a mitocôndria [27].

1.2.1.1. A identidade do MCU

As características moleculares do canal mitocondrial que promove a captação de Ca^{2+} sensível ao *Ruthenium Red* (RR), chamado *MCU* (*Mitochondrial Calcium Uniporter*) vem sendo objeto de muitos trabalhos científicos recentes [32, 33]. A identificação do MCU em nível molecular expandiu uma nova vertente de hipóteses sobre sinalização celular de Ca^{2+} [34]. O canal denominado MCU é formado por um complexo de proteínas. As diversas subunidades proteicas que compõem o canal serão descritas abaixo. Entre as subunidades

está uma proteína também denominada MCU, visto que ela é uma proteína transmembrana e constitui o centro do canal [35, 36].

A ideia de que a proteína MCU é a molécula-chave na captação de Ca^{2+} mitocondrial foi confirmada em uma variedade de sistemas celulares, incluindo o fígado, cardiomiócitos [33, 37], células- β -pancreáticas [38], células cancerosas [39] e neurônios [40]. A proteína MCU é expressa nos organismos, incluindo a maioria dos eucariontes e tecidos humanos com exceção de protistas e fungos [41]. Esta proteína é composta por duas hélices transmembranares ligadas por um seguimento que contém resíduos ácidos denominados DIME [42]. Embora a topologia desta proteína tenha sido inicialmente muito debatida, foi estabelecido que as extremidades amino e carboxil da proteína estão localizadas na matriz [51]; e o seguimento ácido estaria voltado para o espaço intermembrana.

Um parálogo desta proteína é o MCUB, com 50% de identidade (sequência de aminoácidos) e características topológicas semelhantes a MCU. O MCUB são aparentemente não funcionais uma vez que não houve atividade de canal quando a proteína MCUB purificada foi incorporada em bicamadas lipídicas; a sobre-expressão de MCUB em células também não resultou no aumento da captação mitocondrial de Ca^{2+} [43].

O canal MCU é um oligômero formado pela combinação de pelo menos 4 subunidades distintas que já foram descritas, são elas: MICU1, MICU2, MCRU, EMRE (Figura 3) [32]. No entanto, a estequiometria destas subunidades ainda não foi determinada.

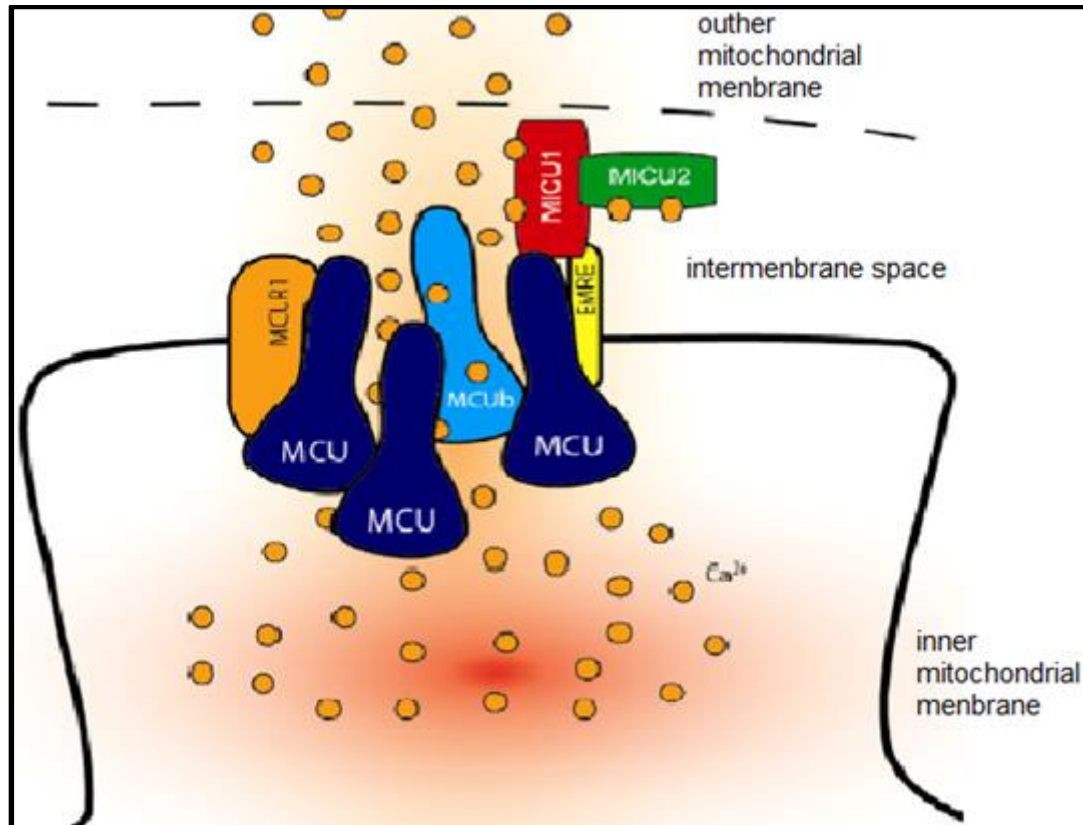


FIGURA 3. Representação do complexo proteico MCU. A captação de Ca^{2+} mitocondrial é controlada por um complexo multiproteico composto por MCU e MCUb (formando o canal de subunidades) em conjunto com EMRE, MICU1, MICU2, MCUR1. Em particular, heterodímeros MICU1/MICU2 atuam como MCU “gatekeeper” devido ao efeito inibitório predominante de MICU2. Adaptado de De Stefani *et al* [44].

A identificação molecular do MCU ocorreu bem recentemente, em 2011. Com a descoberta do MCU, a estrutura central do canal, veio também à descoberta de subunidades reguladoras, que foram mencionadas acima. O MICU1 foi descoberto por Perocchi *et al* [36] e os estudos subsequentes indicaram que o MICU1 tem o papel de modular negativamente a captação de Ca^{2+} mitocondrial [45]. Neste sentido, Mallilankaraman *et al* [46] verificaram que a redução de expressão MICU1 levava a sobrecarga mitocondrial de Ca^{2+} como consequência da atividade “exagerada” do uniporter em condições de repouso da célula. Nesse estudo, o MICU1 pareceu funcionar como limitador da captação de Ca^{2+} mediada por MCU nas concentrações baixas de Ca^{2+} ($<3\mu\text{M}$) típicas de células em estado de repouso. Interessantemente, o MICU1 parece não exercer

tal ação sobre o uniporter quando o mesmo está exposto a altas concentrações de Ca^{2+} [46]. Com base nestes estudos pode-se verificar que o MICU1 tem função de minimizar a atividade do uniporter em condições de repouso, protegendo as mitocôndrias de sobrecarga crônica de Ca^{2+} [47]. Este papel do MICU1 como limitante que previne a sobrecarga de Ca^{2+} mitocondrial pode depender de uma série de variáveis, incluindo o tipo de célula, número e atividade dos canais uniporter em cada mitocôndria e outros mecanismos de regulação [36, 48, 49].

Estudos demonstraram que a alteração da expressão de uma dada subunidades que compõem o complexo MCU podem influenciar os níveis de expressão de outras proteínas componentes do canal, de maneira dependente do tipo de célula [50]. Assim, as interpretações dos experimentos baseados na mudança de expressão de MICU1 são complexos, e os mecanismos pelos quais MICU1 regula a atividade MCU tornou-se confuso e controverso [46, 48]. Há também um desacordo sobre se MICU1 tem ação na regulação da atividade do canal MCU em concentrações de $\text{Ca}^{2+} > 3\mu\text{M}$ [48-51].

O MICU1 foi originalmente pensado ser integral de MMI, porém sua topologia não está totalmente estabelecida de tal modo que ilustrações recentes do complexo de proteínas que formam o MCU não representam esta subunidade de forma inserida na MMI (Figura 3) [36].

O MICU2 tem 27% da identidade de seguimento com MICU1; o MICU2 interage fisicamente com o MICU1 e tem sido sugerido que os dímeros MICU1-MICU2 predominam *in vivo* [51]. Os níveis de expressão da proteína MICU2 dependem da expressão do MICU1 [52]. Existem controvérsias sobre se as mudanças na expressão MICU2 afetam ou não a expressão do MICU1 [51].

MICU2 também parece ser necessário para uma função inibidora sobre a atividade do canal MCU, discutida acima, que tinha sido atribuída ao MICU1. O efeito supressor da

captação mitocondrial de Ca^{2+} de abater a expressão MICU2 foi menor do que os observados quando se abate o MICU1. Assim, tem-se sugerido que a função do MICU1 não requer o MICU2, mas que o inverso não é verdadeiro [52].

O *MCU Regulador 1* (MCUR1) foi descoberto em uma tela de RNAi de genes mitocondriais que regulam captação mitocondrial Ca^{2+} [53]. Este regulador é uma proteína de membrana mitocondrial interna com aproximadamente 40 kD possuindo duas hélices transmembranas com seus terminais amino e carboxil voltados ao espaço intermembrana; há um conector que liga as hélices voltadas a matriz.

O MCUR1 interage fisicamente com a proteína MCU, mas não com o MICU1. MCUR1 tem uma ampla distribuição nos tecidos, sendo que altos níveis de expressão desta proteína são observados no coração [53]. MCUR1 não foi detectado em um estudo proteômico que analisou o complexo do uniporter imunoprecipitado com um epítipo de MCU marcado [54]. Assim, estudos adicionais são necessários para estabelecer os mecanismos e o papel de MCUR1 para a função do complexo proteico do canal MCU.

O *Essencial MCU Regulador* (EMRE) foi descoberto por espectrometria de massa através da análise do proteoma do MCU [54]. É uma proteína de 10 kD com um único domínio transmembrana e com um terminal carboxil altamente ácido. É amplamente expresso nos tecidos de mamífero, e a sua estabilidade é dependente da presença do MCU. A interação de MICU1 e de MICU2 com o MCU é abolida em células quando a expressão de EMRE é reduzida, porém a expressão de MCU permanece inalterada. Assim, a expressão de EMRE é necessária para a atividade do canal MCU mesmo na presença dos outros componentes do uniporter, por mediar a interação de MICU1/2 com MCU [54]. No entanto, MICU1 e MICU2 podem ser co-imunoprecipitados na ausência de EMRE, indicando que a interação MICU1-MICU2 não é dependente de EMRE. Se EMRE medeia todas as interações entre proteínas MICU e MCU ainda não é determinado. É interessante que a

expressão de EMRE está ausente em alguns organismos que expressam MCU, incluindo *Dictyostelium discoideum*. Os detalhes moleculares e a topologia das interações das subunidades proteicas do MCU ainda não são completamente conhecidos [55].

No entanto, se a proteína MCU é por si só suficiente para formar um canal funcional ainda é uma questão em debate. Algumas análises evolutivas de homólogos de MCU e dados experimentais suportam esta hipótese. Por um lado, várias proteínas têm sido descritas como sendo necessárias para a função MCU *in situ*, uma vez que o *knockdown* de MICU1 [36], MCUR1 [53] ou EMRE [56] resultaram na inibição da captação de Ca^{2+} mitocondrial. Por outro lado, partes dos componentes do complexo MCU não são estritamente conservados ao longo da evolução; ex: MCUR1 está presente apenas em metazoários, enquanto plantas e protozoários não apresentam EMRE. Assim, alguns organismos apresentam captação de Ca^{2+} mitocondrial mediada por MCU, mesmo na ausência de EMRE, como foi recentemente demonstrado por Docampo *et al* [57] em tripanossomas.

1.2.2 O efluxo de Ca^{2+} por mitocôndrias

Sabendo que o Ca^{2+} é captado para a matriz mitocondrial através do canal MCU presente na MMI, é presumível que haja um mecanismo de “expulsão” de Ca^{2+} deste compartimento. De fato, a homeostase de Ca^{2+} mitocondrial é auxiliada por dois carreadores independentes que promovem efluxo de Ca^{2+} da organela. Estas duas vias de efluxo são nomeadas como antiporters HCX ($\text{H}^+/\text{Ca}^{2+}$) e NCLX($\text{Na}^+/\text{Ca}^{2+}$).

A ideia de que as mitocôndrias são dotadas de vias de efluxo de Ca^{2+} é explorada desde os anos 70, quando se descobriu que a adição de RR (inibidor do MCU) a mitocôndrias após estas terem acumulado Ca^{2+} , resultava na liberação lenta e praticamente completa deste íon [58-60]. Sugeriu-se que, em mitocôndrias do fígado, os efluxos de Ca^{2+}

é devido a uma troca $2\text{H}^+/1\text{Ca}^{2+}$, processo eletroneutro e de identidade molecular ainda desconhecida [58, 60]. Entretanto, mitocôndrias de coração e outras células excitáveis, tinham um efluxo catalisado por um processo dependente de Na^+ e, por conseguinte, supuseram a existência de um trocador $\text{Na}^+/\text{Ca}^{2+}$ [58]. O efluxo de Ca^{2+} a partir destas mitocôndrias mostra uma dependência sigmoïdal na concentração extramitocondrial de Na^+ (o $K_{0,5}$ desta relação varia entre 10 e 20 μM na maioria dos estudos). Este antiporte por Na^+ é bastante ativo no cérebro, córtex supra-renal e coração [58]. A troca $\text{Na}^+/\text{Ca}^{2+}$ foi relatada pela primeira vez em estudos realizados com uma suspensão de mitocôndrias isoladas a partir do coração [61, 62], posteriormente foi verificada no cérebro, músculo esquelético, glândula parótida e córtex adrenal [58, 63-66]. Nestes tecidos, o efluxo de Ca^{2+} mitocondrial ocorre lentamente na ausência de Na^+ [67].

Em algumas células, principalmente nos hepatócitos, o efluxo de Ca^{2+} dependente de Na^+ é extremamente lento, e a maior parte do efluxo seria depende da troca $\text{H}^+/\text{Ca}^{2+}$.

A identidade molecular deste permutador $\text{Na}^+/\text{Ca}^{2+}$ foi determinada recentemente. O gene do permutador $\text{Na}^+/\text{Ca}^{2+}$ foi identificado por Cai *et al* [68] e Palty *et al* [69], sendo denominado NCLX por ser um termo abreviado para trocador $\text{Na}^+/\text{Li}^+/\text{Ca}^{2+}$; o símbolo do lítio aparece neste nome porque foi constatado que este trocador pode transportar tanto lítio (Li^+) como sódio (Na^+) em troca por Ca^{2+} . Isto difere dos trocadores de membrana plasmática NCX e NCKX, os quais não transportam Li^+ [69].

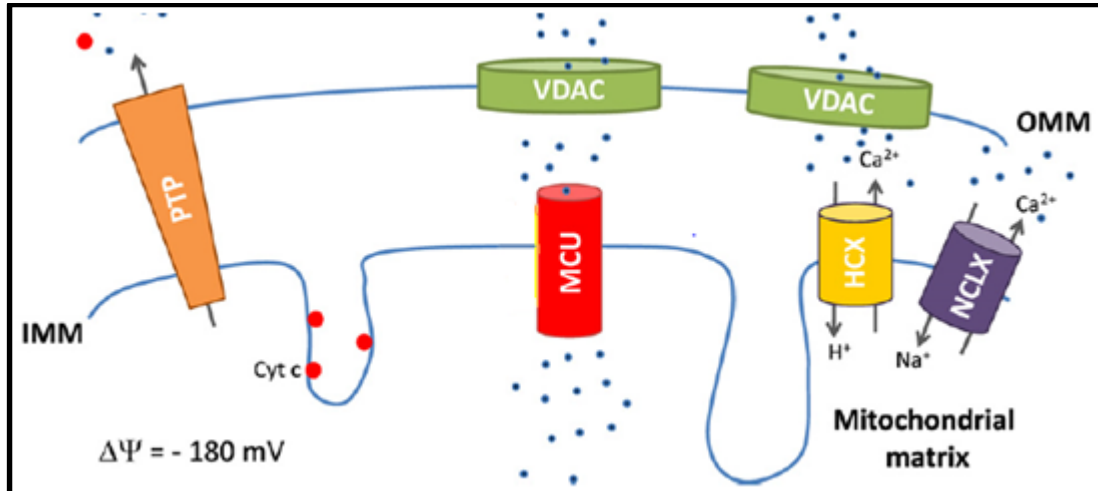


FIGURA 4. Representação esquemática das estruturas proteicas envolvidas no transporte mitocondrial de Ca^{2+} . O transporte mitocondrial de Ca^{2+} ocorre por meio de canais e transportadores localizados na MME e na MMI; o VDAC permite a difusão de Ca^{2+} através da MME; um unipoter eletrogênico (MCU) promove o influxo de Ca^{2+} para a matriz das mitocôndrias; os trocadores $\text{Na}^+/\text{Ca}^{2+}$ (NCLX) e $\text{H}^+/\text{Ca}^{2+}$ (HCX) localizados na MMI são responsáveis pela expulsão do Ca^{2+} da matriz mitocondrial para o espaço intermembranar. Adaptado de Raffaello *et al* 2012 [70].

1.2.3 TRANSIÇÃO DE PERMEABILIDADE MITOCONDRIAL (TPM)

Hunter *et al.* [71] em 1976 expuseram mitocôndrias isoladas ao Ca^{2+} e observaram que o acúmulo mitocondrial deste cátion resultava na permeabilização da organela, devido à formação de um poro na membrana interna. Pelo fato desse processo ser parcialmente revertido através da remoção do Ca^{2+} , esse fenômeno foi denominado “transição de permeabilidade mitocondrial” (TPM) [71, 72].

A TPM é a permeabilização não seletiva da MMI, [73, 74] causada pelo acúmulo excessivo de Ca^{2+} nas mitocôndrias através de um processo estimulado por estresse oxidativo ou por uma variedade de compostos e condições [75-78]. A permeabilização da MMI à H_2O , íons e outras moléculas com peso molecular de até 1500 Daltons [79] que decorre da TPM, resulta em inchamento mitocondrial e ruptura da membrana externa das mitocôndrias [78]. Como consequência direta da permeabilização também ocorre perda do potencial de membrana mitocondrial ($\Delta\Psi$). Devido à disfunção bioenergética da organela e

da liberação de parte de seu conteúdo para o citosol, a TPM pode desencadear a morte celular por apoptose ou necrose.

Apesar de muitas investigações, a natureza molecular do “poro de transição de permeabilidade” (PTP), que é formado na MMI como resultado do processo de TPM, ainda não foi esclarecida [75, 80]. Tem sido sugerido o envolvimento de proteínas da matriz e de proteínas da MME e MMI na composição do PTP - os componentes mais citados são os VDACs, o translocador de nucleotídeo de adenina (ANT), a ciclofilina D (CypD), dentre outras moléculas [81].

Uma concepção preponderante sobre a formação do PTP é de que alterações estruturais em grupos de proteínas da membrana mitocondrial interna levariam à formação de agregados protéicos resultando no PTP da membrana mitocondrial interna [82]. Um mecanismo proposto para a formação do PTP é que altas concentrações de íons de Ca^{2+} e a produção de EROs induziriam a oxidação de resíduos de cisteína e permitiriam a formação de ligações cruzadas de dissulfeto (S-S) [82, 83].

A TPM é inibida pela ciclosporina A (CsA) na faixa nano molar; esta droga é um peptídeo cíclico de 11 aminoácidos lipofílicos com um peso molecular de 1,202 kDa, descoberto em 1970 através de um programa de busca para antibióticos e antifúngicos iniciados em 1958 [84]. A CsA possui uma elevada afinidade de ligação com a ciclofilina (CypD) [85]. A CypD está localizada na matriz mitocondrial e possui atividade enzimática peptidil-prolil-isomerase (PPI-ase), que é essencial para o dobramento de proteínas *in vivo*. A ligação de CsA a CypD inibe a sua atividade PPI-ase.

Em 1987, Fournier e colaboradores [86] foram os primeiros a estudar a interação da CsA com a mitocôndria isolada. Eles verificaram que a CsA inibiu a respiração mitocondrial e também bloqueou o efluxo de Ca^{2+} da mitocôndria. Eles estabeleceram a hipótese de que a CsA poderia inibir o efluxo de Ca^{2+} mitocondrial e que a abertura reversível do PTP poderia

mediar esse efluxo de Ca^{2+} [87, 88]. Seguindo outra linha, Crompton e colaboradores [89] investigaram primeiro se a CsA poderia inibir a abertura do PTP e observaram que a abertura do PTP nas mitocôndrias isoladas de coração de ratos induzida pela adição de Ca^{2+} e fosfato poderia ser inibida por CsA (60 CsA $\text{pmol}\cdot\text{mg}^{-1}$ de proteína mitocondrial).

O mecanismo pelo qual a CsA inibe a abertura do PTP só foi revelado em um estudo posterior, em 1990 [90]. Este estudo relatou que CsA inibia a abertura do PTP por ligar-se a CypD; os dados apresentados e a argumentação eram: já se sabia que a CsA se ligava a CypD dentro da célula [91]; estudos demonstraram que existia uma CypD mitocondrial [92]; o K_i encontrado de CsA para CypD e a inibição do PTP ocorreram em faixas de concentrações semelhantes (i.e. ~ 5 nM); e, por fim, os números de sítios de ligação da CsA envolvidos na inibição do PTP nas mitocôndrias do fígado e do coração foram muito próximos da quantia de CypD presentes na matriz mitocondrial [90]. Um aspecto importante e de relevância fisiológica é que a ocorrência da TPM é inibida por nucleotídeos de adenina [93].

2.OBJETIVOS

- Avaliar o transporte de Ca^{2+} na presença e ausência de CsA em diferentes concentrações de Ca^{2+} externo.
- Avaliar o transporte de Ca^{2+} e a atividade respiratória de mitocôndrias isoladas de diferentes tecidos de ratos machos e fêmeas sob condições experimentais que impedem a ocorrência de TPM induzida por Ca^{2+} :
 - fígado;
 - músculo esquelético;
 - coração;
 - cérebro.

3. CAPÍTULO

Research article

Tissue and sex specificities in the Ca²⁺ handling by isolated mitochondria: Evaluations under conditions avoiding the permeability transition

Hanan Chweih, Roger F. Castilho, Tiago R. Figueira

Department of Clinical Pathology, Faculty of Medical Sciences, State University of Campinas, Campinas, Brazil.

Abstract

The characteristics of mitochondria, including their Ca²⁺ transport functions, may exhibit tissue specificity and sex dimorphism. Because the measurements of the Ca²⁺ handling by isolated mitochondria may be biased by dysfunction secondary to Ca²⁺-induced mitochondrial permeability transition (MPT) pore opening, this study evaluates the extent to which MPT inhibition by cyclosporine-A affects the measurement of Ca²⁺ transport in isolated rat liver mitochondria. The results indicate that the steady-state levels of external Ca²⁺ and the rates of mitochondrial Ca²⁺ efflux through the selective pathways can be overestimated by up to 4-fold if MPT pore opening is not prevented. Then, we analyzed the Ca²⁺ transport in isolated mitochondria from the liver, skeletal muscle, heart and brain of male and female rats under incubation conditions containing MPT inhibitors, NAD-linked substrates and relevant levels of free Ca²⁺, Mg²⁺ and Na⁺. The Ca²⁺ influx rates were similar among the samples, except for the liver mitochondria displaying values 4-fold higher. In contrast, the Ca²⁺ efflux rates exhibited more tissue diversity, especially in the presence of Na⁺. Interestingly, the Na⁺-independent Ca²⁺ efflux was highest in the heart mitochondria (~4 nmol/mg/min), thus challenging the view that heart mitochondrial Ca²⁺ efflux relies almost exclusively on a Na⁺-dependent pathway. Sex specificity was only observed in two kinetic indexes of heart mitochondrial Ca²⁺ homeostasis and in the ADP-stimulated respiration of liver mitochondria (~20% higher in females). The present study shows the

Physiological diversity in mitochondrial Ca²⁺ transport

methodological importance of preventing MPT when measuring the properties and the physiological variability of the Ca²⁺ handling by isolated mitochondria.

Keywords: mitochondrial calcium uniporter, mitochondrial calcium transport, mitochondrial permeability transition, calcium homeostasis, mitochondrial ion exchange

Abbreviations: CsA, cyclosporin A; IMM, inner mitochondrial membrane; MCU, mitochondrial Ca²⁺ uniporter; MPT, mitochondrial permeability transition; MRT, mean response time; NCLX, sodium/lithium/calcium exchanger; RR, ruthenium red.

Introduction

Recent landmark discoveries about the molecular identities of integral proteins that handle the Ca²⁺ movement across the inner mitochondrial membrane (IMM) have boosted interest in this field (3, 5, 13, 14, 33).

The current view of mitochondrial Ca²⁺ handling must include the major latest findings, such as *i*) the molecular identification of the mitochondrial Ca²⁺ uniporter (MCU) (13), an IMM protein complex whose function had been electrophysiologically characterized as a fast channel responsible for Ca²⁺ influx into the mitochondrial matrix (28); *ii*) the genetic engineering of mice that are born alive and thrive despite lacking MCU activity (33); and *iii*) the molecular identification of the Na⁺/Ca²⁺ exchanger (NCLX), the main pathway for mitochondrial Ca²⁺ efflux in excitable cells (5, 32).

The mitochondrial Ca²⁺ transport system plays the physiological role of transferring cytosolic Ca²⁺ transients into changes in the free and total Ca²⁺ levels in the mitochondrial matrix (35, 47). This transport process can promote both the accumulation of Ca²⁺ within mitochondria and the shaping of the cytosolic Ca²⁺ signal. A main factor that determines the mitochondrial Ca²⁺ accumulation is the dynamic balance between the rates of Ca²⁺ influx

Physiological diversity in mitochondrial Ca²⁺ transport

and efflux (*i.e.*, the net Ca²⁺ flux) across the IMM (35). Notably, a mitochondrial Ca²⁺ overload may trigger the so-called Ca²⁺ induced permeability transition (MPT) pore opening, a cellular event that contributes to many pathophysiological processes (18). In functional energized (*i.e.*, polarized) mitochondria, energy-driven net Ca²⁺ uptake and retention occur whenever the Ca²⁺ levels in the vicinity of the organelle are sufficiently high to support MCU-mediated influx rates higher than the efflux rates mediated by Na⁺-independent and Na⁺-dependent pathways (18, 35, 47). In turn, Na⁺-dependent mitochondrial Ca²⁺ efflux occurs through the integral protein NCLX with electrogenic Na⁺/Ca²⁺ antiport (32), whereas Na⁺-independent Ca²⁺ efflux operates at slower rates than the former and occurs via an exchange with H⁺ (22, 23, 31). The activities of these two Ca²⁺ efflux pathways are thought to display great tissue heterogeneity (11, 23), but some results from early studies might have been biased by non-experimentally controlled Ca²⁺-induced MPT pore opening during the assays (4, 20-22, 48). Indeed, data indicate that measurements of mitochondrial Ca²⁺ efflux kinetics are affected by modulators of MPT pore opening (20, 22, 46, 49). Intact isolated heart mitochondria exposed to a moderate Ca²⁺ load of ~60 nmol Ca²⁺/mg of protein exhibited Ca²⁺ efflux rates that were slower in the presence of the MPT inhibitor cyclosporin A (CsA) (46). Similar results were observed by others when MPT was inhibited by adenine nucleotides or transgenic Bcl-2 overexpression (20, 22, 48, 49). However, inhibitors such as adenine nucleotides or CsA have not been commonly used to prevent undesired Ca²⁺-induced MPT pore opening in *in vitro* assays that evaluate mitochondrial Ca²⁺ handling, despite the fact that CsA was characterized as a potent inhibitor of Ca²⁺-induced MPT in 1988 (9).

The heterogeneity of mitochondrial Ca²⁺ influx across tissues is also an issue that lies between differing experimental conditions and techniques (24). The most insightful findings with regard to mitochondrial Ca²⁺ uptake heterogeneities across tissues were obtained in an electrophysiological study that observed very low MCU activity in heart

Physiological diversity in mitochondrial Ca²⁺ transport

organelles compared with that in liver, kidney, skeletal muscle and brown adipose tissue mitochondria (17); the latter two tissues exhibited similar MCU activities, which were also the highest measured MCU activities. Nonetheless, because of the complex nature of MCU-mediated mitochondrial influx, its assessments are highly dependent on experimental conditions. For example, the presence of Mg²⁺ as a physiological inhibitor of MCU and the changes in membrane potential across the IMM that accompany fast mitochondrial Ca²⁺ influx will be important modulators of the Ca²⁺ influx rate in *in situ* organelles (16, 24, 36, 37). The changes in electrical differences across the IMM caused by Ca²⁺ influx are prevented in electrophysiological studies, and in physiological conditions, these changes are counteracted by the activity of the respiratory chain, which exhibits tissue specificity and dependence on energizing substrates (42). Some mitochondrial characteristics may also display sex dimorphism in rats. The liver mitochondrial respiratory activity and its transcriptional regulation differ between male and female rats (8, 25). Because of all of these issues, different studies are hardly comparable, and fundamental questions about mitochondrial Ca²⁺ influx and efflux properties in respiring organelles and their tissue specificities remain unclear.

In this scenario, we aimed to evaluate Ca²⁺ transport in respiring (at the expense of NAD-linked substrates) mitochondria isolated from the liver, heart, brain and skeletal muscle of female and male rats while preventing the undesirable bias of MPT pore opening that leads to mitochondrial dysfunction. Our linear and exponential analysis of Ca²⁺ fluxes across the IMM under suitable conditions provided these highlighted findings: *i*) MPT inhibition does indeed affect measurements of Ca²⁺ transport variables; *ii*) mitochondrial Ca²⁺ transport variables vary substantially by tissue type but not sex, with the exception of two assessed variables that differed between female and male heart mitochondria; *iii*) heart mitochondria exhibit a substantial rate of Na⁺-independent Ca²⁺ efflux and an unexpected small

Physiological diversity in mitochondrial Ca²⁺ transport

stimulation by Na⁺; and *iv*) liver and heart mitochondria respectively exhibit the highest and lowest kinetic tendency of accumulating Ca²⁺, as evidenced by their Ca²⁺ influx:efflux ratios that differ by nearly 100-fold.

Materials and Methods

Animals and Reagents: Wistar rats (HanUnib:WH) from CEMIB UNICAMP (Campinas, SP, Brazil) were maintained in the animal facility of our department. The rats were housed at 22 ± 2 °C on a 12-h light-dark cycle with free access to a standard laboratory rodent chow diet (Nuvital CR1, Nuvital, Curitiba, PR, Brazil) and tap water. Groups of 3- to 4-month-old male and female rats were used for the measurements described below after euthanasia by decapitation. The animal procedures were approved by the local Committee for Ethics in Animal Experimentation at the university (#2897-1) and are in accordance with the Guide for the Care and Use of Laboratory Animals published by the National Academy of Sciences. Unless otherwise stated, all utilized chemicals were of the highest grade and purchased from Sigma (St. Louis, MO, USA).

Mitochondrial isolation and incubation conditions: Mitochondria from the liver, heart, and brain were isolated by conventional differential centrifugation as described previously (27, 39, 40). Mitochondria isolation from skeletal muscle was as follows: quadriceps samples were trimmed from connective tissue and finely diced with scissors in ~20 mL of isolation medium I (100 mM sucrose, 50 mM KCl, 50 mM Tris, 5 mM EDTA, 1 mM K₂HPO₄, and 2 g/L BSA; pH 7.4). Then, the samples were subjected to 2 x 3" homogenization in an Ultra-Turrax T25 (Wilmington, NC, USA) operating at 11,000 rpm and transferred to a glass potter (Kontes Glass #23, Vineland, NJ, USA) for a further 8-stroke homogenization against a loose motor-driven Teflon pestle. The homogenate was then suspended in 40 mL and centrifuged at 800g for 10 min to obtain a clear supernatant that

Physiological diversity in mitochondrial Ca²⁺ transport

was collected after the floating white layer was discarded. This supernatant was subsequently centrifuged at 10,000g for 10 min, and the resulting pellet containing mitochondria was suspended gently in isolation medium I with the aid of a tiny paint brush. The suspension was centrifuged again at 10,000g for 10 min, and the pellet was rinsed twice with fresh changes of isolation medium II (225 mM mannitol, 75 mM sucrose, and 10 mM Tris; pH 7.4) prior to its suspension in 50 μ L of the same medium with the gentle procedure described above. The entire isolation procedure was conducted on ice or at 4 °C. The protein concentrations of the final mitochondrial suspensions were determined using a modified Biuret assay. Unless otherwise stated, all experiments with isolated mitochondria were performed at 28 °C in a standard reaction medium containing 125 mM sucrose, 65 mM KCl, 2 mM K₂HPO₄, 1 mM free Mg²⁺, 20 μ M EGTA, and 10 mM HEPES buffer at pH 7.2 and supplemented with a cocktail of NAD-linked substrates (5 mM malate, 5 mM α -ketoglutarate, 5 mM pyruvate, and 5 mM glutamate) prior to use. None of the reagents was a sodium salt, nor was NaOH used to titrate the pH; thus, the Na⁺-independent mitochondrial Ca²⁺ efflux could be measured.

Respirometry: Oxygen consumption was measured using an OROBOROS Oxygraph-2k (Innsbruck, Austria) in 2 mL of standard reaction medium supplemented with 200 μ M EGTA. After measurements of the basal O₂ consumption (State II respiration), stimulated respiration by oxidative phosphorylation (State III respiration) was elicited by the addition of saturating levels of ADP (300 μ M for liver and 500 μ M for the others samples); then, 1 μ g/mL oligomycin was added to inhibit the phosphorylation by ATP synthase and obtain the resting leak respiration (State IV). The final concentrations of mitochondrial proteins in the assay were 0.25 (skeletal muscle and heart mitochondria) or 0.5 mg/mL (liver and brain mitochondria).

Physiological diversity in mitochondrial Ca²⁺ transport

Calibration of Ca²⁺ Indicator Probe: Analysis of the free Ca²⁺ levels outside the mitochondria were obtained by monitoring the fluorescence of the probe Calcium GreenTM-5N (Molecular Probes, Invitrogen, Carlsbad, CA, USA) over time using a spectrofluorometer (Shimadzu RF-5301, Kyoto, Japan) operating at excitation and emission wavelengths of 506 and 532 nm, respectively. The dissociation constant (K_d) of the probe Calcium GreenTM-5N was determined under our incubation conditions from a calibration curve with varying concentrations of free Ca²⁺ that was built with reciprocal dilutions between solutions A and B. Solution A was the standard reaction medium containing 0.2 μM Calcium GreenTM-5N, and solution B was solution A plus 1.2 mM CaCl₂. The total calcium content of solutions A and B was measured using atomic absorption spectroscopy, and the free Ca²⁺ levels of the reciprocally diluted curve were calculated using WEBMAXC STANDARD (available <http://web.stanford.edu/~cpatton/webmaxcS.htm>). From the determined K_d of 25 μM for Calcium GreenTM-5N under our conditions, the raw fluorescence readings measured during mitochondrial Ca²⁺ transport assays were converted into Ca²⁺ concentration levels (in μM) according to the manufacturer's hyperbolic equation: $[Ca^{2+}] = 25 * ((F - F_{min}) / (F_{max} - F))$, where F is any given fluorescence value, F_{min} is the lowest fluorescence reading after the addition of 0.5 mM EGTA, and F_{max} is the maximal fluorescence obtained after two sequential additions of 1 mM CaCl₂. F_{min} and F_{max} were determined using an internal calibration procedure at the end of all recordings of the traces of Calcium GreenTM-5N fluorescence, as represented in **Fig. 1A**. For the Mg²⁺-free experimental conditions, the K_d was changed to 20 μM.

Measurement of mitochondrial Ca²⁺ transport variables: Ca²⁺ movements across the IMM were measured in mitochondria that were incubated in 2 mL of standard reaction medium supplemented with 0.2 μM Calcium GreenTM-5N and MPT inhibitors (1 μM CsA plus 200 μM ADP and 1 μg/mL oligomycin for assays with brain mitochondria or 1 μM CsA alone for measurements with the mitochondria from the other tissues). CaCl₂ was added to the

Physiological diversity in mitochondrial Ca²⁺ transport

reaction medium prior to the beginning of the trace recording to establish the desired free Ca²⁺ concentrations ranging from 7 to 42 μM , as detailed in the figure legends. As indicated by the representative experiment shown in **Fig. 1A**, mitochondria were added to a final concentration of 0.5 mg/mL (liver and brain samples) or 0.25 mg/mL (heart and skeletal muscle samples) right after the start of the fluorescence measurement; after asymptotic fluorescence values were obtained, the MCU inhibitor ruthenium red (RR) and NaCl were sequentially added to a final concentration of 1 μM and 15 mM, respectively. Thereafter, the fluorescence signal was calibrated and transformed into free Ca²⁺ levels as described above. The four different phases (named a, b, c and d in **Fig. 1B**) of the free Ca²⁺ concentration-time data plot were best fitted to linear (phases a, b and c) and exponential (phase d) functions (OriginPro 8.0, Origin Lab, Northampton, MA, USA) to yield the kinetic variables of mitochondrial Ca²⁺ transport. The slopes of the linear functions were taken as the mitochondrial rates of initial net Ca²⁺ uptake (phase a), Na-independent Ca²⁺ efflux (phase b) and Na-present Ca²⁺ efflux (phase c). The duration of phase a was either the first three seconds after the addition of the sample to the assay for liver and muscle mitochondria or the first ten seconds for brain and heart mitochondria; thus, these time windows represent a similar percentage of the full amplitude of the mitochondrial influx response among the organelles from different tissues. Phase d of the Ca²⁺ transport curve, which is the monoexponential decay of external Ca²⁺ levels and their asymptotic values, was fitted to the following exponential equation (ExpDecay1, OriginPro 8.0): $y = y_0 + A_1 * e^{-(x-x_0)/t1}$, where the estimated equation parameters y_0 , A_1 and $t1$ represent the Ca²⁺ levels at the asymptote (in μM), the full amplitude of the exponential decay response (in μM) and the mean response time (MRT, expressed in seconds) of the exponential influx response, respectively. Notably, MRT is a valuable kinetic parameter that reveals the time spent to cover 63% of the amplitude of the response (A_1 , or the total change in Ca²⁺ concentration), and multiplying

Physiological diversity in mitochondrial Ca²⁺ transport

MRT by 4.6 provides the time to cover the entire amplitude of the response (A_T) and reach the asymptotic values (19).

To analyze the dependence of the Ca²⁺ influx rate on the external Ca²⁺ concentration within a single Ca²⁺ transport curve, exponentially fitted data from phase d were plotted as a function of time, and the instant rates of Ca²⁺ influx were determined using the first derivative of Y ($d[Ca^{2+}]/dt$), as detailed in **Fig. 1C**. Then, the $d[Ca^{2+}]/dt$ (in $\mu M/s$) data were normalized by volume and protein to show the net influx rate (in nmol/mg/min) plotted against the levels of external free Ca²⁺, as indicated in the example in **Fig. 1D**. The slope of the linear relationship between net Ca²⁺ influx rate and the external free Ca²⁺ concentration (**Fig. 1D**) was taken as the response of the Ca²⁺ influx rate to changes in the external Ca²⁺ levels and is expressed in nmol/mg/min/ μM .

An estimate of the steady-state $[Ca^{2+}]$ (the asymptotic Y value of its decay curve over time) in the presence of 15 mM Na⁺ was calculated based on our measured rates of Ca²⁺ efflux in the absence and presence of 15 mM Na⁺ and on the dependence of the net Ca²⁺ influx rate on the external $[Ca^{2+}]$ (*i.e.*, the relationship described in **Fig. 1D**), according to the equation $e[Ca^{2+}]_{ss} = ((sodium-Ca^{2+}_{EFFLUX} - Ca^{2+}_{EFFLUX})-a)/b$, where $e[Ca^{2+}]_{ss}$ is the estimated steady-state $[Ca^{2+}]$ in the presence of 15 mM Na⁺, $sodium-Ca^{2+}_{EFFLUX}$ is the measured Ca²⁺ efflux rate in the presence of 15 mM Na⁺, Ca^{2+}_{EFFLUX} is the measured Ca²⁺ efflux rate in the absence of Na⁺, and **a** and **b** are the linear and the angular coefficients, respectively, of the linear regression obtained in the analyses exemplified in **Fig. 1D**. This calculation is derived from the kinetic fact that the Na⁺ addition increases the mitochondrial Ca²⁺ efflux rate and that a new steady-state of $[Ca^{2+}]$ will be attained when the gross Ca²⁺ influx rate also increases to balance the current Ca²⁺ efflux supported by Na⁺. Therefore, upon Na⁺ addition, a new net Ca²⁺ flux equal to zero must occur at a higher concentration of external Ca²⁺.

Physiological diversity in mitochondrial Ca²⁺ transport

Statistical Analysis: Data are reported as the mean \pm SEM. The sample size is given in the figure legends. Repeated two-way ANOVA was conducted using SPSS software (v. 17.0, SPSS Inc., Chicago, IL, USA), and repeated one-way ANOVA with the FISCHER-LSD post hoc test was performed using Statistica software (Statistica 7.0, Stat Soft, Tulsa, OK, USA) when appropriate. Non-parametric data were tested with Friedman ANOVA followed by Wilcoxon pair analyses with *P*-corrected values (Statistica 7.0) [50].

Physiological diversity in mitochondrial Ca^{2+} transport

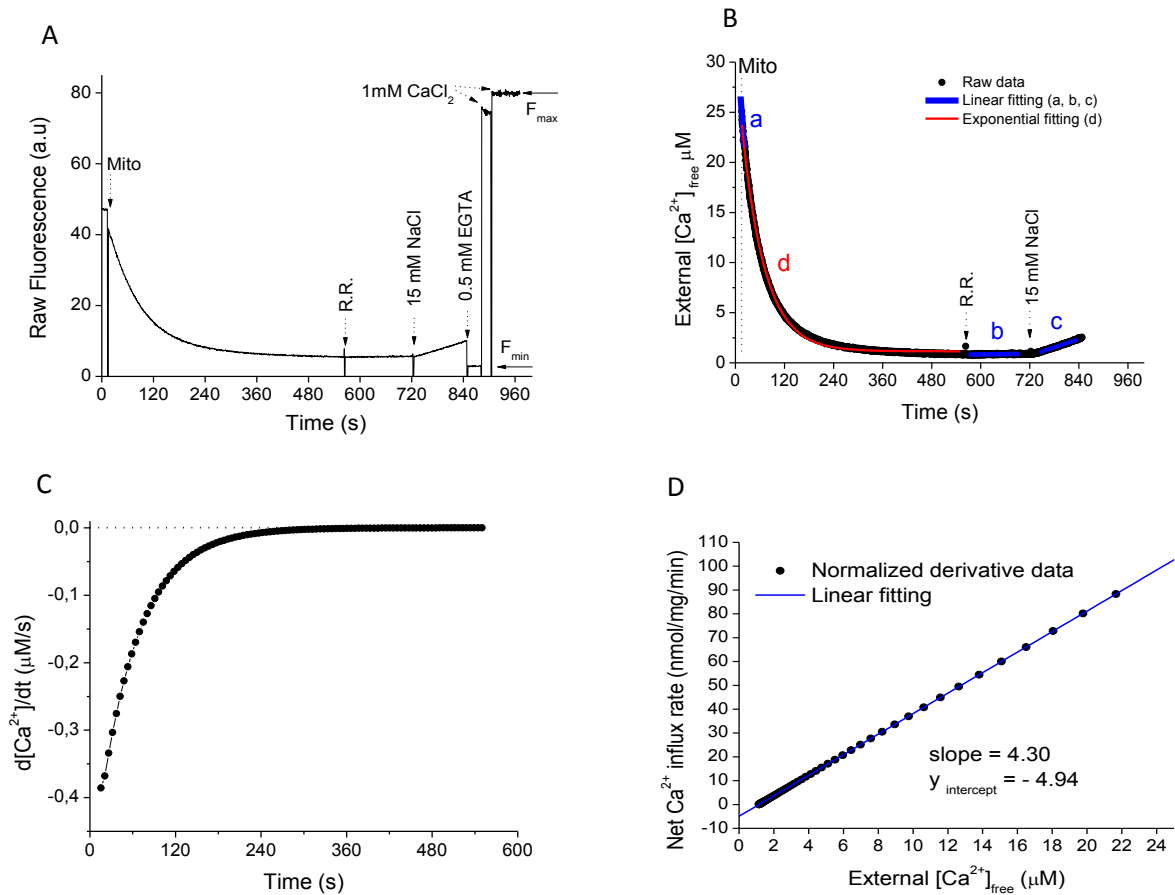


Fig. 1. Example of the assessment of mitochondria Ca^{2+} transport variables with the use of a fluorescent probe. Panel A depicts the addition of a sample of isolated skeletal muscle mitochondria (Mito; 0.25 mg/mL) to 2 mL of basic incubation medium supplemented with 0.2 μM Calcium GreenTM-5N, MPT inhibitor (1 μM CsA) and an initial free $[\text{Ca}^{2+}]$ of 20 μM while the fluorescence levels were monitored over time. After the addition of mitochondria and the attainment of steady-state fluorescence levels, 1 μM ruthenium red (RR), 15 mM NaCl, 0.5 mM EGTA and 1 mM CaCl_2 (added twice) were added where indicated; as described in the Materials and Methods, the fluorescence signal was transformed into free $[\text{Ca}^{2+}]$ levels (μM) and plotted against time (panel B). Panel B shows four different phases of the $[\text{Ca}^{2+}]$ decay curve, referred to as a, b, c and d, that were best fitted to linear (phases a, b and c) and exponential (phase d) equations. The slopes of phases a, b and c provided the initial mitochondrial Ca^{2+} influx rate, the Na^+ -independent Ca^{2+} efflux rate and the Na^+ -present Ca^{2+} efflux rate, respectively. The exponential fitting of phase d yielded the following variables: Ca^{2+} levels at the asymptote (in μM), the full amplitude of the exponential decay response (in μM) and the mean response time (MRT, measured in seconds) of the exponential influx response. Panel C shows the first-order derivative of the fitted values of phase d as a measure of the instant rates of mitochondrial Ca^{2+} influx that were then corrected for protein and volume and plotted against their respective external free $[\text{Ca}^{2+}]$ in panel D. The slope of the linear fitting of the curve shown in panel D was taken as the response of the Ca^{2+} influx rate.

Results

Effects of MPT inhibition by CsA on the measurement of Ca²⁺ handling by isolated liver mitochondria.

In the first part of our study, we evaluated whether MPT inhibition by CsA during a mitochondrial Ca²⁺ transport assay would affect the measurements of selected variables that describe handling of Ca²⁺ by mitochondria (**Figs. 2 and 3**) isolated from liver. The Ca²⁺ influx rate is dependent on the initial Ca²⁺ levels, which also determine the mitochondrial Ca²⁺ load and the propensity for Ca²⁺-induced MPT; thus, four different initial [Ca²⁺] were used. In contrast to the two lowest [Ca²⁺] of 7 and 11 μM, the two highest concentrations of 20 and 42 μM clearly led to opening of the MPT pore in the control conditions (*i.e.*, absence of CsA), as evidenced by mitochondrial Ca²⁺ release instead of the asymptotic phase (**Fig. 2A**) that should follow the net Ca²⁺ influx phase. When the mitochondrial Ca²⁺ transport was assayed in the presence of CsA, there was no indication of MPT pore opening across the range of initial Ca²⁺ levels (**Fig. 2B**). Mitochondrial Ca²⁺ efflux rates were not calculated when MPT-mediated Ca²⁺ efflux was evident, which included the control conditions of 20 and 42 μM for the initial [Ca²⁺]; likewise, the determination of the initial Ca²⁺ influx rate was also precluded at the 42 μM [Ca²⁺] control condition. A dashed vertical line was drawn in the bar graphs of **Figs. 2 and 3** to indicate that control conditions represented on the right led to MPT pore opening. Exactly as shown in **Fig. 1**, the initial Ca²⁺ influx rate (**Fig. 2C**) and the Na⁺-independent (Fig. 2D) and Na⁺-present Ca²⁺ (**Fig. 2E**) efflux rates were determined by linear analyses. The initial Ca²⁺ influx rates did not differ between the conditions at the [Ca²⁺] tested (**Fig. 2C**), even at 20 μM [Ca²⁺] where MPT occurred in the control condition (**Fig. 2B**). As expected, the influx rates increased non-linearly with increasing initial Ca²⁺ levels. The Na⁺-independent Ca²⁺ efflux was significantly lower in the CsA condition than in the control;

Physiological diversity in mitochondrial Ca²⁺ transport

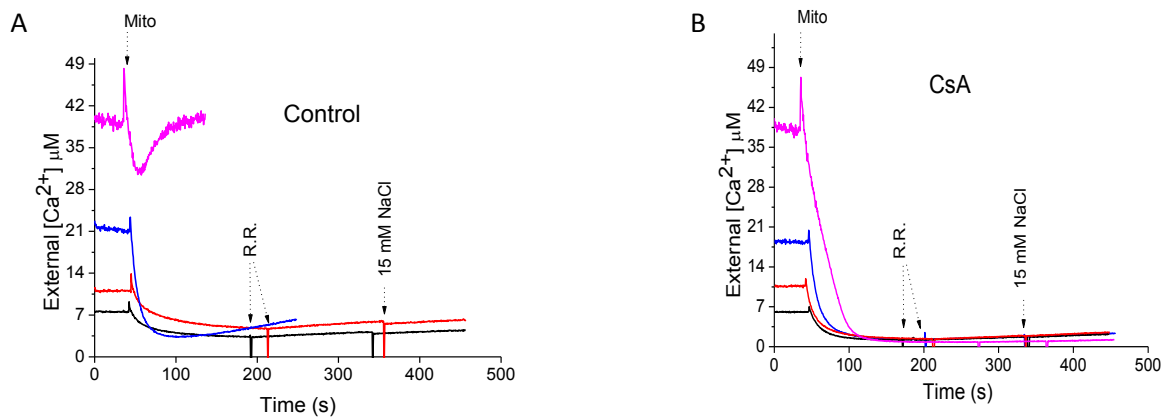
additionally, as the initial [Ca²⁺] increased, the efflux rates increased and decreased in the control and CsA conditions, respectively (**Fig. 2D**). Surprisingly, these effects of CsA on the efflux rate are much less prominent in the presence of Na⁺, although the effect was statistically significant for the condition with an initial [Ca²⁺] of 11 μM (**Fig. 2E**). Such phenomena arise from the fact that the addition of Na⁺ to the system led to unchanged or decreased Ca²⁺ efflux rates under the control conditions at 7 and 11 μM for the initial [Ca²⁺]; in contrast, the Na⁺ addition stimulated the Ca²⁺ efflux rates in the presence of CsA at all tested initial Ca²⁺ levels (**Fig. 2F**).

As the greatest effects of CsA on mitochondrial Ca²⁺ efflux were observed at an 11 μM initial [Ca²⁺] (**Fig. 2D**), we sought to study whether another inhibitor of MPT would provide similar results to CsA at this Ca²⁺ concentration. For this purpose, the mitochondrial Ca²⁺ efflux rates were evaluated in the standard reaction medium supplemented with 1 μg/mL oligomycin to inhibit phosphorylation by mitochondrial ATP synthase while either 1 μM CsA or 200 μM ADP was used to inhibit MPT during the assay. From this protocol using ADP as an MPT inhibitor, the Na⁺-independent and Na⁺-present Ca²⁺ efflux rates (in nmol/mg/min) were 1.22 ± 0.26 and 0.78 ± 0.14 in the control condition, 0.32 ± 0.04 and 0.39 ± 0.07 in the CsA condition, and 0.33 ± 0.06 and 0.36 ± 0.07 in the ADP condition, respectively.

From these experiments with liver mitochondria under the control and CsA conditions, exponential fits of the [Ca²⁺] decay curve provided the kinetic variables shown in **Fig. 3**. The external Ca²⁺ levels at the steady state (*i.e.*, asymptote) were significantly lower in the CsA conditions than in the controls at 11 and 20 μM initial [Ca²⁺] (**Fig. 3A**); in contrast to the results in the control conditions, the steady-state [Ca²⁺] decreased as the initial [Ca²⁺] increased in the presence of CsA. The response of the Ca²⁺ influx rates to the changes in the external Ca²⁺ levels differed between control and CsA conditions and across Ca²⁺ levels (**Fig. 3B**); this variable was obtained from single Ca²⁺ decay curves shown in **Fig. 1D** and is

Physiological diversity in mitochondrial Ca^{2+} transport

a valuable kinetic parameter that may reflect both the affinity and the activation of the MCU-mediated mitochondrial Ca^{2+} uptake process. The overall kinetics of net Ca^{2+} uptake by mitochondria was taken as the MRT (time to cover 63% of the entire amplitude of the exponential Ca^{2+} decay curve), and CsA made this MRT shorter only at an initial $[\text{Ca}^{2+}]$ of 7 μM (**Fig. 3C**). We also normalized the MRT by the amplitude of the exponential decay response (**Fig. 3D**) because CsA changed the steady-state $[\text{Ca}^{2+}]$ (**Fig. 3A**) and thus the amplitude and because the initial Ca^{2+} level itself determine the amplitude. However, this approach only helped to reveal that increasing the initial Ca^{2+} levels dramatically accelerated the overall net mitochondrial Ca^{2+} uptake towards the attainment of the asymptote. When MPT was prevented by CsA, strong and significant correlations were observed between MRT and the steady-state $[\text{Ca}^{2+}]$ (**Fig. 3E**). In contrast, it is quite interesting that this relationship is lost if the MPT pore opening is not inhibited during the assay (**Fig. 3F**).



Physiological diversity in mitochondrial Ca^{2+} transport

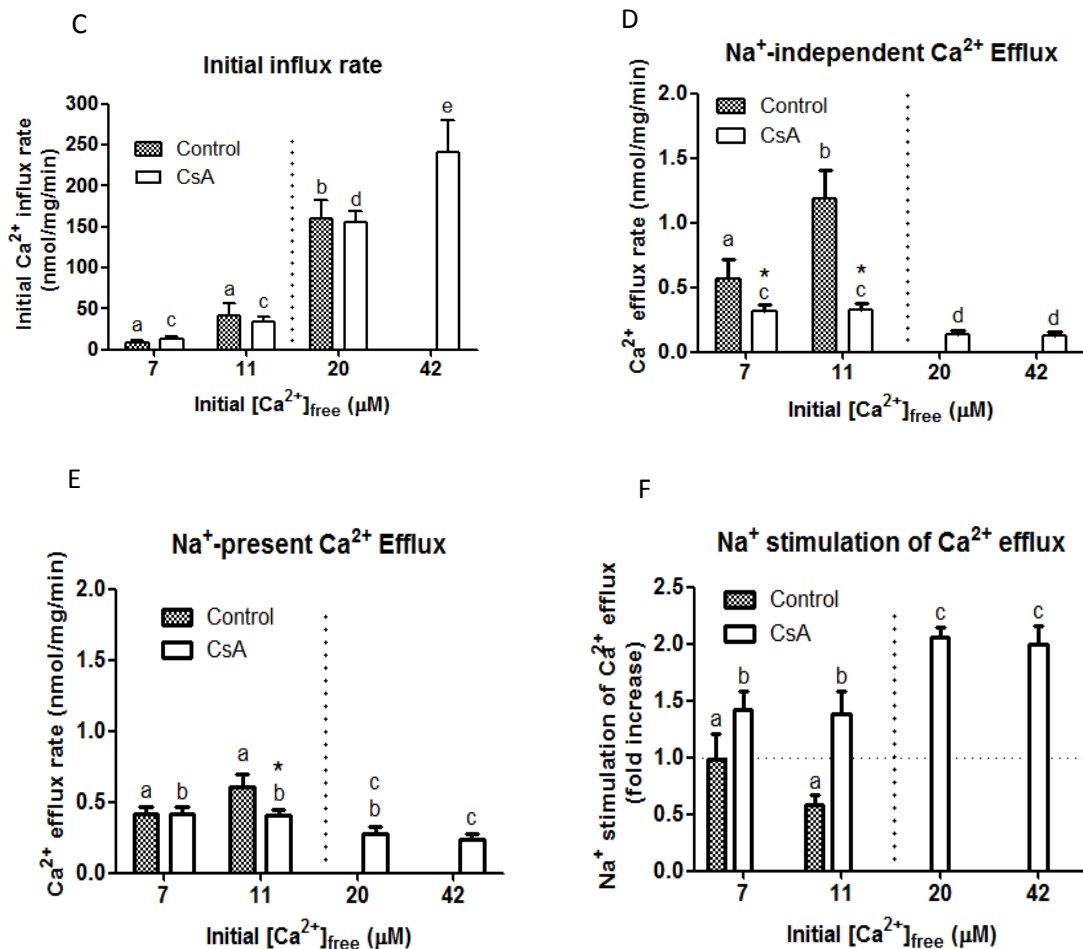


Fig. 2. Effects of MPT inhibition by CsA on the Ca^{2+} transport rates in isolated liver mitochondria. Variables (mean \pm SEM, N = 5 each group) were assessed at different initial $[\text{Ca}^{2+}]$, as shown on the abscissa of the bar graphs, and in the absence (Control) and presence of 1 μM CsA, an MPT inhibitor. Within a condition (e.g., control or CsA), the bars that do not share the same letter are different from each other; *difference between conditions at the same $[\text{Ca}^{2+}]$. The Ca^{2+} concentrations on the right side of the vertical dashed lines in the bar graphs clearly elicited MPT in the control condition, as evidenced by the Ca^{2+} release rather than asymptote in the $[\text{Ca}^{2+}]$. Under such conditions, the measurement of some variables was avoided to prevent bias. Data were statistically tested for within-subject factors using a repeated two-way ANOVA followed by a paired *t*-test or using a one-way repeated ANOVA with Fisher-LSD post hoc tests within a single factor when the F ratio was significant in the previous two-way ANOVA. Representative curves of mitochondrial Ca^{2+} transport assessed at varying initial $[\text{Ca}^{2+}]$ and in the absence (Control) and presence of CsA are shown in **Panel A** and **Panel B**, respectively; the additions of mitochondria sample (Mito; 0.5 mg/mL), 1 μM ruthenium red (RR) as an MCU inhibitor and 15 mM NaCl are indicated in the graphs by arrows. **Panel C:** initial rate of net mitochondrial Ca^{2+} influx; the main effects found using ANOVA were significant for the initial $[\text{Ca}^{2+}]$. **Panel D:** rate of mitochondrial Ca^{2+} efflux in the absence of Na^+ ; the ANOVA main effects were significant for the initial $[\text{Ca}^{2+}]$, CsA presence and interaction. **Panel E:** rate of mitochondrial Ca^{2+} efflux in the presence of 15 mM Na^+ ; the ANOVA main effects were significant for CsA presence; **Panel F:** the stimulation of Ca^{2+} efflux from mitochondria promoted by Na^+ , calculated as the ratio between the data shown in panels D and E.

Physiological diversity in mitochondrial Ca^{2+} transport

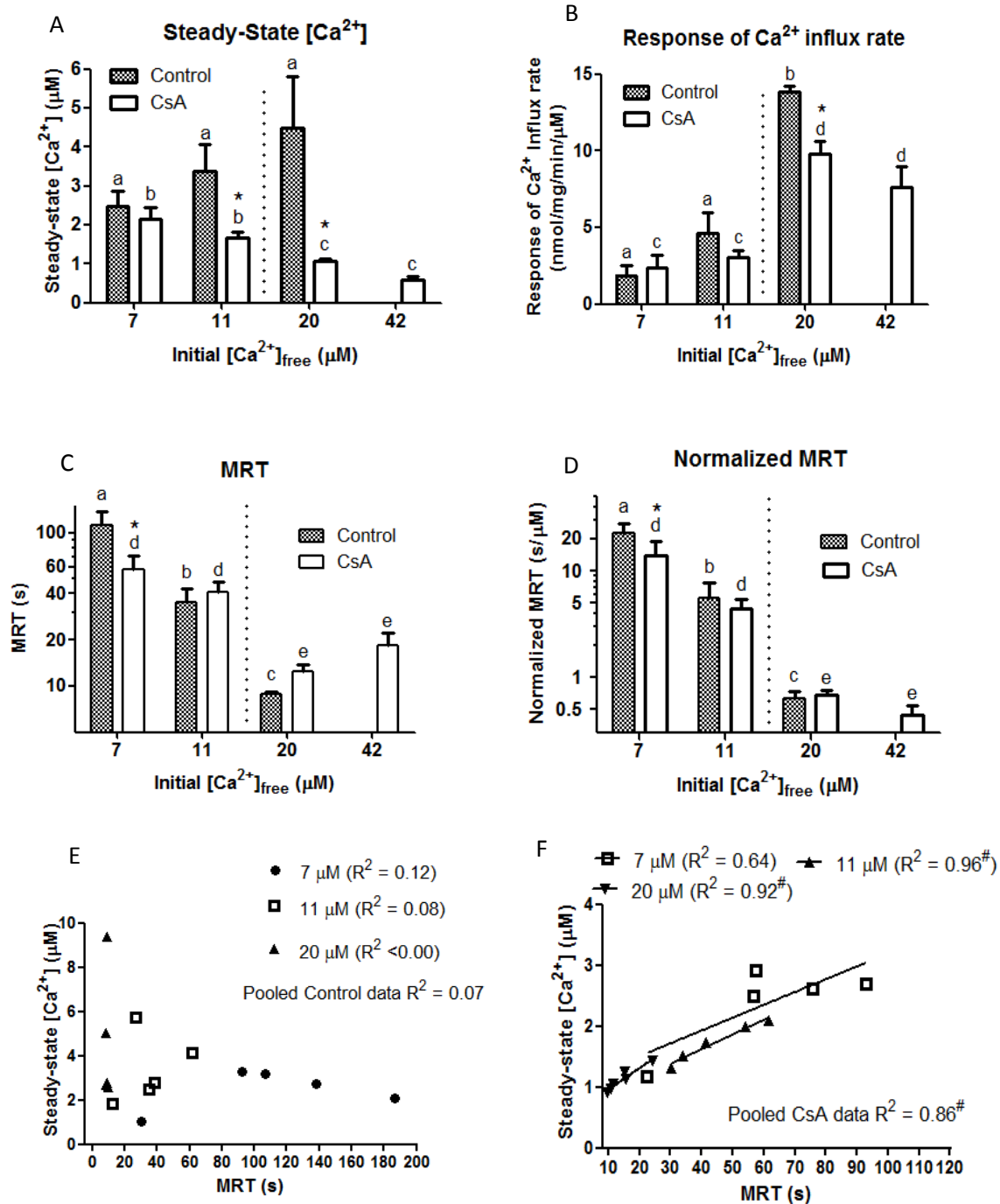


Fig. 3. Effects of MPT inhibition by CsA on the overall kinetics of net Ca^{2+} uptake by isolated liver mitochondria. Variables (presented as the mean \pm SEM, $N = 5$) were assessed at different initial $[\text{Ca}^{2+}]$, as shown on the abscissa, and in the absence (Control) and presence of 1 μM cyclosporine A (CsA), an MPT inhibitor. Within a condition (e.g., control or CsA), the bars that do not share the same letter are different from each other; *difference between conditions at the same $[\text{Ca}^{2+}]$. The Ca^{2+} concentrations on the right side of the vertical dashed lines clearly elicited MPT in the control condition, as evidenced by the Ca^{2+} release rather than asymptote $[\text{Ca}^{2+}]$. Under such conditions, the measurement of some variables was avoided to prevent bias.

Physiological diversity in mitochondrial Ca²⁺ transport

Data (except for panel C) were statistically tested for within-subject factors using a repeated two-way ANOVA followed by a paired *t*-test or using one-way repeated ANOVA with Fisher-LSD post hoc tests within a single factor when the F ratio was significant in the previous two-way ANOVA. Data from panel C were statistically tested using Friedman ANOVA followed by Wilcoxon pair analyses with *P*-corrected values. **Panel A:** The steady-state Ca²⁺ concentration was determined from the asymptote of the exponential fitting; the ANOVA main effects were significant for CsA presence; **Panel B:** response of mitochondria Ca²⁺ influx rate to changes in external [Ca²⁺] as determined in **Fig. 1C**; the ANOVA main effects were significant for initial [Ca²⁺], CsA presence and interaction; **Panel C:** the mean response time (MRT) of the net mitochondrial Ca²⁺ uptake determined as the *t*₁ parameter of the exponential fitting equation is shown on the y axis using a logarithmic scale; the ANOVA main effects were significant for [Ca²⁺]; **Panel D:** amplitude normalized mean response time (*t*₁/*A*₁ from the exponential fitting equation) of the net mitochondrial Ca²⁺ uptake shown on the y axis using a logarithmic scale; **Panel E:** Correlation between the steady-state [Ca²⁺] and the MRT determined in the control condition. **Panel F** Correlation between the steady-state [Ca²⁺] and the MRT determined in the presence of CsA, #*P* ≤ 0.05 .

Sex and tissue diversity in mitochondrial functions.

After we understood the effects of CsA-induced MPT inhibition on the variables describing the mitochondrial Ca²⁺ handling in organelles isolated from the liver, we then investigated the tissue and sex specificities of mitochondrial Ca²⁺ transport while preventing the undesirable effects secondary to MPT pore opening. Mitochondria were isolated from the liver, skeletal muscle, heart and brain of male and female rats for subsequent determination of the respiratory activity and Ca²⁺ transport variables in the presence of MPT inhibitors. The oxygen consumption rates under respiratory states II, III and IV exhibited significant differences between tissues (**Fig. 4A-C**), whereas the ADP-respiratory control ratios did not differ (**Fig. 4D**). The mitochondria from heart and skeletal muscle displayed faster rates than those of the liver and brain organelles. Sex only affected the state III respiration rate (*i.e.*, ADP-stimulated respiration) in the liver mitochondria: the rate was ~20% higher (*P* ≤ 0.05) in females than in males (**Fig. 4B**). The initial rate of mitochondrial Ca²⁺ influx was nearly 5-fold higher (*P* ≤ 0.05) in the liver than in the organelles from the skeletal muscle, heart or brain, which presented rates similar to each other (**Fig. 5A**); a similar tissue pattern was also observed for the response of the Ca²⁺ influx rate shown in **Fig. 5B**. None of these two mitochondrial Ca²⁺ influx variables differed between the sexes.

Physiological diversity in mitochondrial Ca²⁺ transport

The mitochondrial Ca²⁺ efflux mediated by the putative H⁺/Ca²⁺ exchanger, which is termed the Na⁺-independent Ca²⁺ efflux in the present paper, exhibited similar rates in the mitochondria from the liver, skeletal muscle and brain; all of these rates were slower than 0.5 nmol/mg/min. Surprisingly, the efflux through this pathway in the heart mitochondria was nearly 4 nmol/mg/min and was significantly higher ($P \leq 0.05$) than that in the organelles from the other tissues (**Fig. 5C**). When Na⁺ is present, Na⁺/Ca²⁺ exchange can occur via NCLX; in this case, the mitochondria from all tissues exhibit Ca²⁺ efflux rates that differ from each other ($P \leq 0.05$), with the highest rates observed in the heart, followed by the skeletal muscle, brain and liver organelles (**Fig. 5D**). The extent to which Na⁺ stimulated the mitochondrial Ca²⁺ efflux over the rates in the absence of Na⁺ is shown in **Fig. 5E**; this variable also varied substantially between tissues ($P \leq 0.05$).

As an index of the balance between mitochondrial Ca²⁺ influx and efflux, which could translate into a dynamic tendency of mitochondria to accumulate Ca²⁺ upon a cytosolic Ca²⁺ transient, we calculated the ratio between the initial Ca²⁺ influx and the Na⁺-present efflux rates (**Fig. 5F**). This ratio varied widely ($P \leq 0.05$) across tissues, with the liver organelles displaying the highest average values of approximately 500 and values as low as 4 in the heart and nearly 21 and 13 in the skeletal muscle and brain mitochondria, respectively.

The asymptote in the [Ca²⁺] decay curve represents a null rate of net mitochondrial Ca²⁺ influx. Conceivably, mitochondria only accumulate Ca²⁺ when the Ca²⁺ level outside the organelle is greater than this steady-state concentration. The Ca²⁺ levels at this steady state were determined in the mitochondria from the four tissues and are shown in **Fig. 5G**. The steady-state [Ca²⁺] significantly differed across tissues with the highest values in the heart and brain, where the values significantly exceeded those in the skeletal muscle and liver; however, the only difference in the steady-state [Ca²⁺] between the sexes was the higher value in the heart mitochondria of females compared with those in males ($P \leq 0.05$).

Physiological diversity in mitochondrial Ca²⁺ transport

Kinetically, the steady-state [Ca²⁺] will increase as the gross influx rate decreases or the gross efflux rate increases. Because Na⁺ stimulated Ca²⁺ efflux from the mitochondria of all studied tissues, we calculated the extent ($\epsilon\Delta$, estimated change) of the increase in the steady-state [Ca²⁺] when mitochondrial Ca²⁺ efflux is stimulated by Na⁺ (**Fig. 5H**); this increase ranged between 0.5 and 1.2 μM Ca²⁺ across tissues but did not differ significantly.

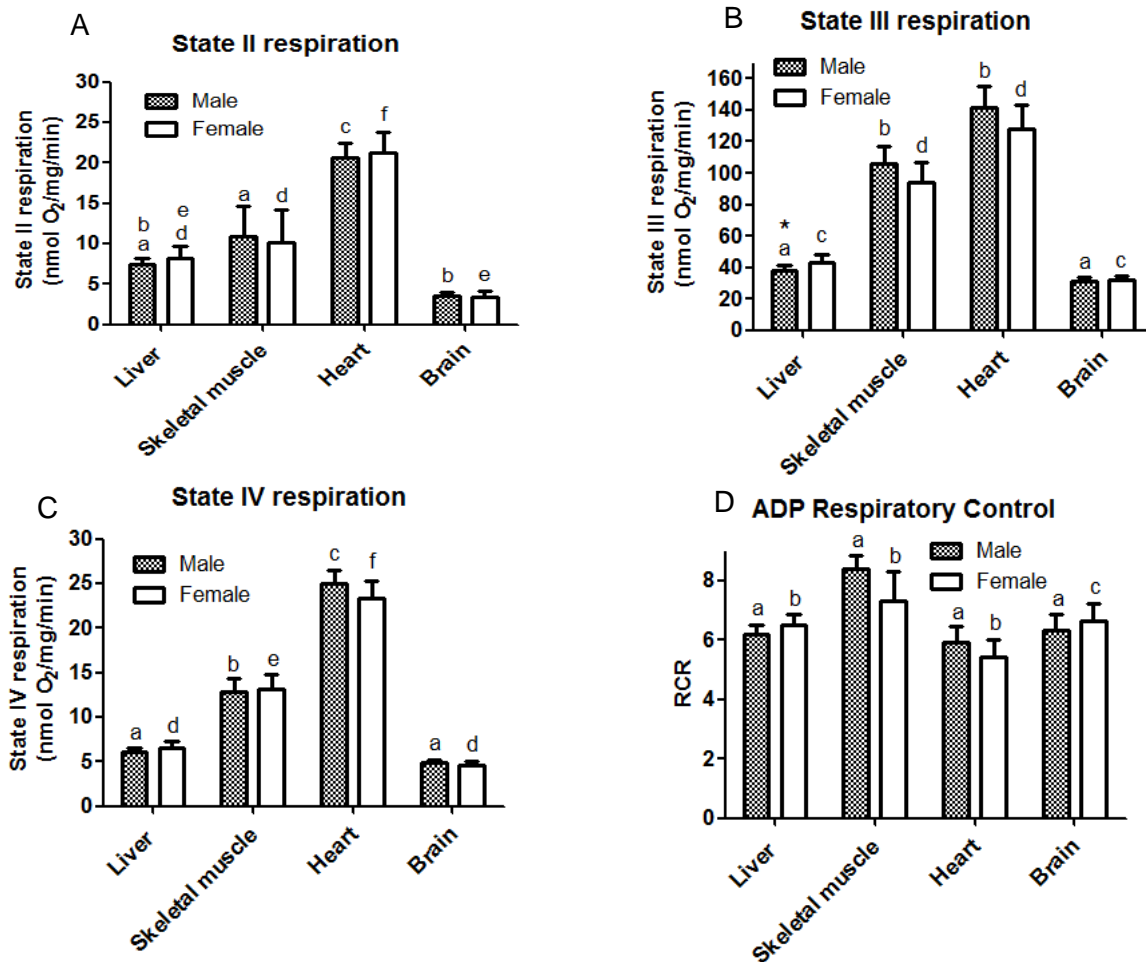
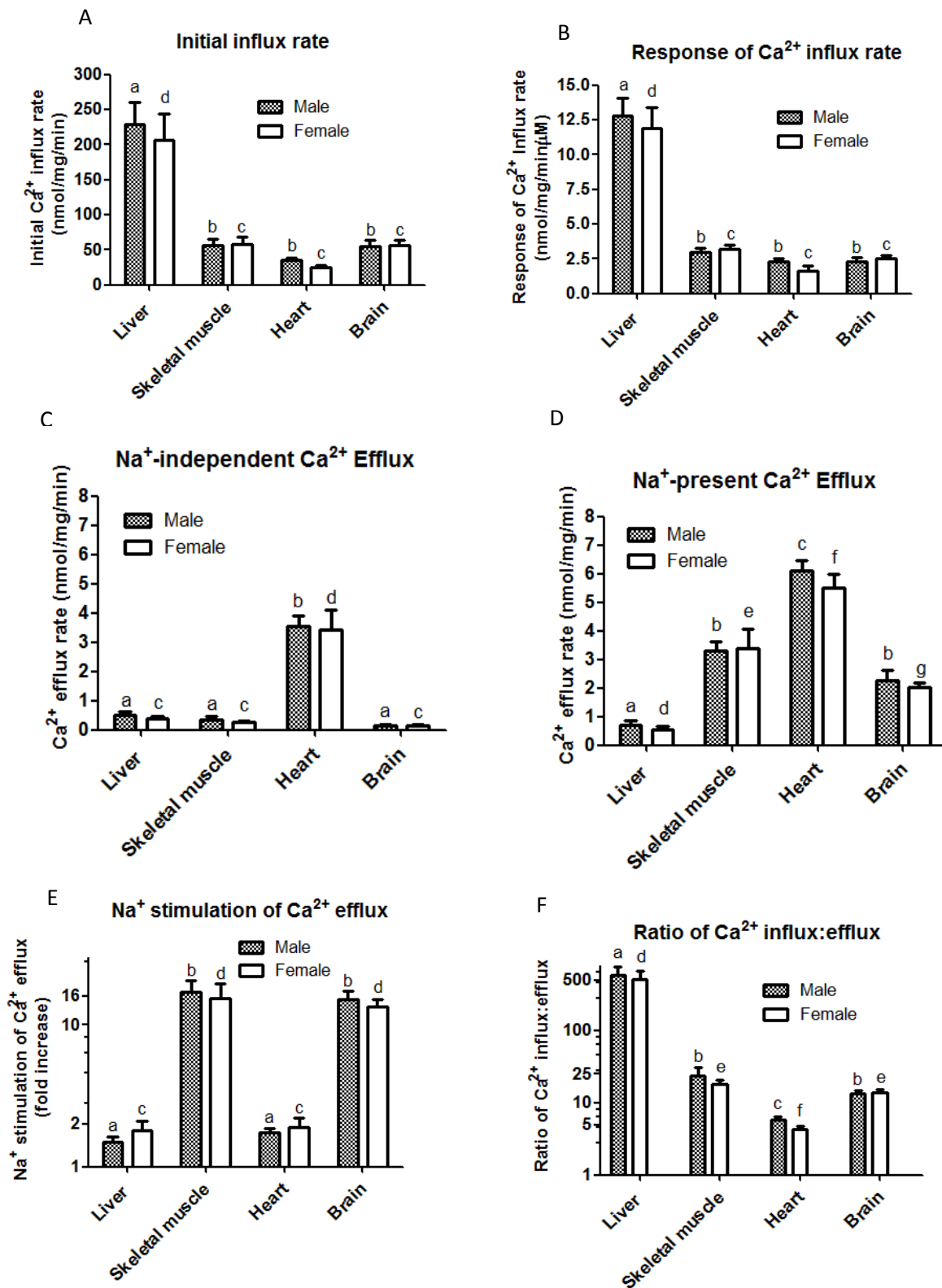


Fig.4. Respiratory activities of isolated mitochondria from the liver, skeletal muscle, heart and brain of male and female rats. The variables (presented as the mean \pm SEM, N = 5-11) of all samples were obtained from isolated mitochondria incubated in the same basic medium supplemented with 200 μM EGTA. The bars that do not share the same letters within a given sex are different from each other; *different ($P \leq 0.05$) from the same female tissue. Data (except for the panel B and D data that were tested using the Kruskal-Wallis and Wilcoxon test) were statistically tested using repeated two-way ANOVA followed by Fisher-LSD post hoc tests. **Panel A:** State II respiration, basal respiratory rate in the absence of exogenous ADP. **Panel B:** State III respiration, respiratory rate in the presence of saturating ADP levels to induce oxidative phosphorylation. **Panel C:** State IV respiration, respiratory activity following the cessation of phosphorylation as induced by the addition 1 $\mu\text{g}/\text{mL}$ oligomycin to the system. **Panel D:** respiratory control by ADP calculated as the ratio of the State III: State IV rates.

Physiological diversity in mitochondrial Ca^{2+} transport



Physiological diversity in mitochondrial Ca^{2+} transport

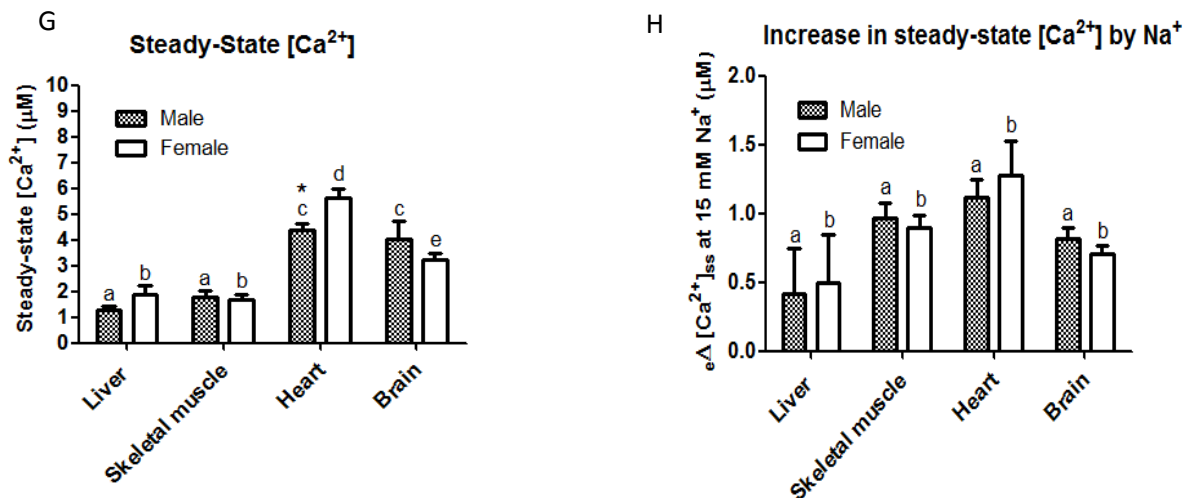


Fig. 5. Ca^{2+} handling by isolated mitochondria from liver, skeletal muscle, heart and brain of male and female rats. Variables were assessed in all samples as detailed for **Fig. 1** with the initial free $[\text{Ca}^{2+}]$ set at 20 μM and in the presence of MPT inhibitors. Data are presented as the mean \pm SEM, $N = 5-8$; the bars that do not share the same letter within the same sex are different from each other; *different ($P \leq 0.05$) from the same female tissue. Data (except for panels E, F and H) were statistically tested using repeated two-way ANOVA followed by Fisher-LSD post hoc tests; data from panels E, F and H were tested using the Kruskal-Wallis test across tissues and the Wilcoxon test between sex pairs. **Panel A:** initial net mitochondrial Ca^{2+} influx rate. **Panel B:** response of the mitochondria Ca^{2+} influx rate to changes in the external $[\text{Ca}^{2+}]$ as determined in Fig. 1C; **Panel C:** mitochondrial Ca^{2+} efflux in the absence of Na^+ ; **Panel D:** mitochondrial Ca^{2+} efflux in the presence of 15 mM Na^+ ; **Panel E:** Na^+ stimulation of mitochondrial Ca^{2+} efflux, calculated as the ratio between the data from panels C and D are shown on the y axis using a logarithmic scale. **Panel F:** ratio between the rates of initial Ca^{2+} influx and Na^+ -present Ca^{2+} efflux; **Panel G:** steady-state $[\text{Ca}^{2+}]$ determined as the asymptote of the exponential fit; **Panel H:** estimated increase in steady-state $[\text{Ca}^{2+}]$ induced by the Na^+ -stimulated mitochondrial Ca^{2+} efflux

The exponential fittings of the $[\text{Ca}^{2+}]$ decay curve from all tissue mitochondria provided the time constant MRT; this variable describes the overall kinetics of the net mitochondrial Ca^{2+} uptake (**Fig. 6**). MRT is not linearly related to mitochondrial content (21), and thus, we did not perform statistical comparisons across tissues, which could be misleading in the homeostatic viewpoint. Similarly to most of the mitochondrial Ca^{2+} -handling variables measured in the present study, MRT did not differ between males and females, but a non-significant trend ($P = 0.09$) was observed in the heart mitochondria (**Fig. 6A**). A slower MRT in female heart mitochondria would be consistent with the significantly higher steady-state $[\text{Ca}^{2+}]$ that was also observed in the female heart mitochondria because there may be a strong positive correlation between these two variables, at least in the liver (**Fig. 3E**). In fact,

Physiological diversity in mitochondrial Ca²⁺ transport

when the MRT was normalized by the amplitude of the entire influx response, a significant ($P \leq 0.05$) sex difference arose in the heart mitochondria, with female organelles exhibiting a slower response than males (**Fig. 6B**).

There is a general belief that the Ca²⁺ efflux from heart mitochondria relies almost exclusively on Na⁺/Ca²⁺ exchange (35); nonetheless, most of the previous reports on the Ca²⁺ efflux from heart mitochondria consist of studies using succinate as an energizing substrate and an assay media devoid of Mg²⁺. Thus, we attempted to evaluate whether the unexpected high rate of Na⁺-independent heart mitochondrial Ca²⁺ efflux observed here (**Fig. 5D**) could be related to differences in the assay conditions. When we removed Mg²⁺ from the medium and replaced the cocktail of NAD-linked substrates used throughout this study with succinate plus rotenone as an energizing substrate, the Na⁺-independent and the Na⁺-present mitochondrial Ca²⁺ efflux rates were 1.03 ± 0.17 and 31.0 ± 4.17 nmol/mg/min, respectively (**Fig. 7**). Notably, this finding very closely resembles the widely known high Na⁺ stimulation of Ca²⁺ efflux from heart mitochondria. Heart mitochondrial Ca²⁺ efflux was also assayed under incubation conditions containing NAD-linked substrates but devoid of Mg²⁺; thus, the roles of energizing substrate and Mg²⁺ in determining the Ca²⁺ efflux rate could be better understood (**Fig. 7**). It was evident that the chosen substrates (a cocktail of NAD-linked substrates vs. the FAD-linked succinate) were the main factors underlying our findings (*i.e.*, the relatively high Na⁺-independent and relatively low Na⁺-present Ca²⁺ efflux rates from heart mitochondria). Ruling out the possibility that the stock solution of NAD-linked substrates cocktail contained Na⁺ from any source, we remind the reader that the same stock solution of substrates was used in the assays with skeletal muscle and brain mitochondria, which do exhibit Ca²⁺ efflux rates that are highly stimulated by NaCl addition (**Fig. 5E**).

Physiological diversity in mitochondrial Ca^{2+} transport

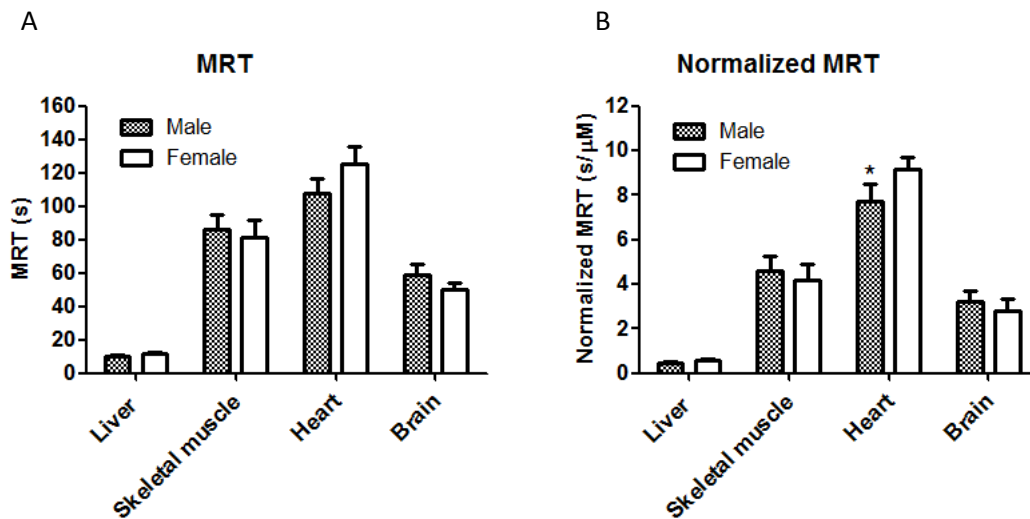


Fig. 6. Overall kinetics of the net Ca^{2+} uptake by isolated mitochondria from the liver, skeletal muscle, heart and brain of male and female rats. The variables were assessed in all samples as detailed for **Fig. 1** with the initial free $[\text{Ca}^{2+}]$ set at $20 \mu\text{M}$ and in the presence of MPT inhibitors. Only sex effects were statistically tested using a paired t-test and the Bonferroni P -corrected value. *significantly different from the same female tissue. Comparisons between different tissues were not made; these comparisons could be misleading with regard to understanding the mitochondrial Ca^{2+} handling *in situ* because the MRT is non-linearly proportional to the mitochondrial content, which is known to differ between different cell types. **Panel A:** the mean response time (MRT) of the net mitochondrial Ca^{2+} uptake determined as the t_1 parameter from the exponential fit. **Panel B:** amplitude normalized mean response time (t_1/A_1 , both from the exponential fit) of the net mitochondrial Ca^{2+} uptake.

Physiological diversity in mitochondrial Ca^{2+} transport

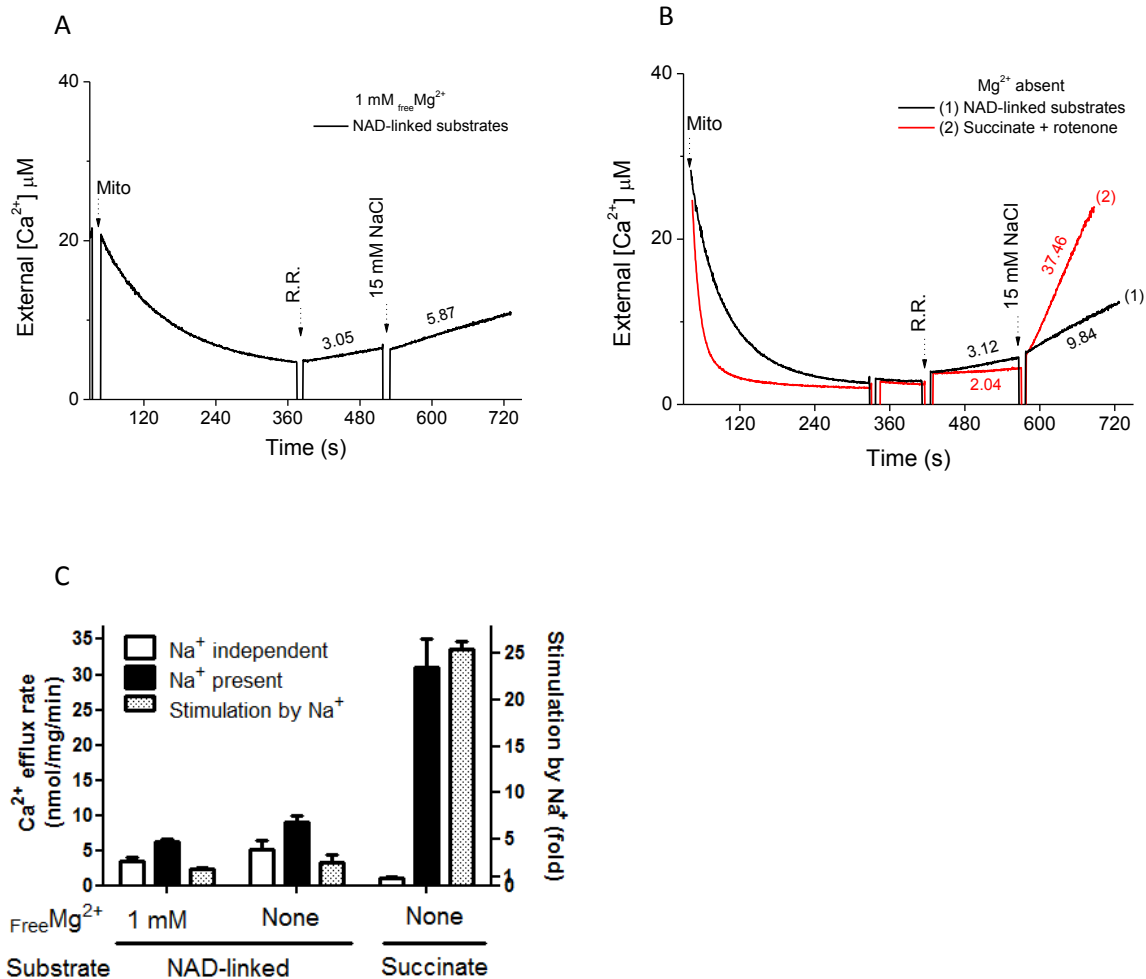


Fig. 7. Ca^{2+} efflux rates from isolated heart mitochondria are dependent on exogenous substrates. Panel A: a representative curve of a Ca^{2+} transport assay with male rat heart mitochondria under the standard incubation condition containing NAD-linked substrates (5 mM each of malate, glutamate, and pyruvate α -ketoglutarate) and 1 mM free Mg^{2+} , as detailed in the Materials and Methods section. **Panel B:** representative curves of a Ca^{2+} transport assay of isolated male rat heart mitochondria energized by either NAD-linked substrates or 10 mM succinate plus rotenone (1 μM) in a reaction medium devoid of Mg^{2+} . The mitochondrial sample (0.25 mg/mL), 1 μM ruthenium red (RR), and 15 mM NaCl were added where indicated; the numbers next to the trace are the efflux rates in nmol/mg/min. **Panel C** depicts the mean \pm SEM values (N = 5) of the Na^{+} -independent and Na^{+} -present Ca^{2+} efflux rates (in nmol/mg/min) of heart mitochondria under the three different incubation conditions; the ratio between these two rates accounts for the stimulation of Ca^{2+} efflux induced by Na^{+} and is presented as the right y axis variable.

Discussion

The data presented here address an unsettled question about tissue and sex diversities in mitochondrial Ca^{2+} transport. The novelty and importance of the presented findings stem from the following: *i)* investigations of the sex dimorphism for mitochondrial Ca^{2+} transport in different tissues; *ii)* experimental conditions tailored for physiologically relevant levels of free Ca^{2+} , Mg^{2+} and Na^{+} ; and *iii)* the avoidance of undesirable effects that are secondary to Ca^{2+} -induced MPT during *in vitro* assays. Due to uncertainties about whether and/or to what extent uncontrolled MPT may affect the measurement of each mitochondrial Ca^{2+} transport variable, the first part of this study aimed to directly address this intriguing question that has emerged from accumulating findings since the 1980s (4, 46, 48, 49).

Effects of MPT inhibition by CsA on the measurement of mitochondrial Ca^{2+} handling.

MPT pore opening with varying conductance states may occur in isolated mitochondria loaded with Ca^{2+} . Although MPT itself may be considered a mechanism involved in mitochondrial Ca^{2+} homeostasis in intact cells (15), high Ca^{2+} loads promptly lead to the opening of high-conductance MPT pore and irreversible mitochondrial dysfunction in isolated organelles that are studied in the absence of endogenous MPT inhibitors, such as adenine nucleotides (30, 41). Therefore, it is conceivable that if the MPT is not prevented during assays involving Ca^{2+} -exposed mitochondria, the resulting loss of organelle integrity could bias measurements of the variable of interest. In fact, the data obtained here (**Figs. 2 and 3**) indicate that MPT inhibition by CsA alters the measurement of Ca^{2+} -handling variables even at low Ca^{2+} levels (*i.e.*, 7 and 11 μM). Under conditions of higher Ca^{2+} levels (*i.e.*, 20 and 42 μM) in the absence of CsA, MPT clearly ensues and promotes Ca^{2+} release

instead of steady-states levels (**Figs. 2A** and **2B**). Among the commonly measured Ca^{2+} transport variables, only the initial rates of mitochondrial Ca^{2+} influx (determined in a 3-s window) were not affected by the CsA inhibition of MPT regardless of the initial Ca^{2+} level, which corroborates the findings from a study of isolated heart mitochondria exposed to $\sim 15 \mu\text{M}$ Ca^{2+} (46). Additionally, non-linear analyses show that the presence of CsA in the assay does not exert main effects on the overall mitochondrial Ca^{2+} uptake kinetics (**Figs. 3B-D**). Nonetheless, the steady-state $[\text{Ca}^{2+}]$ and the mitochondrial Ca^{2+} efflux rates in the absence and presence of Na^+ were significantly lower in the presence of CsA, and this effect depended on the initial Ca^{2+} levels (*i.e.*, the higher the initial $[\text{Ca}^{2+}]$ was, the higher the effect of CsA). A lower mitochondrial Ca^{2+} efflux rate in the presence of CsA has been observed previously by others, but that finding was not interpreted in light of the MPT inhibition by this drug (46). Strengthening the role of MPT instead of off-target CsA effects, the replacement of CsA by ADP, an MPT inhibitor, resulted in rather similar effects with regard to Na^+ -independent and Na^+ -present mitochondrial Ca^{2+} efflux rates, and these effects are consistent with previous findings (20, 22, 48). One of the most insightful results in terms of the importance of avoiding MPT pore opening during Ca^{2+} transport assays is reported in Figs. 2F, 3E and 3F. A 50 to 100% stimulation of liver mitochondrial Ca^{2+} efflux by Na^+ is only observed when the assay medium contains CsA, and Na^+ can even inhibit the Ca^{2+} efflux in the control condition (**Fig. 2F**). Thus, the widespread concept that the Ca^{2+} efflux from liver mitochondria does not involve the $\text{Na}^+/\text{Ca}^{2+}$ exchanger is challenged by the data obtained under experimental conditions that prevent MPT pore opening.

The steady-state Ca^{2+} levels represent a dynamic null balance between the gross rates of mitochondrial Ca^{2+} influx and efflux. Accordingly, a decreased Ca^{2+} efflux rate will be balanced by a decreased gross mitochondrial Ca^{2+} influx supported by lower levels of external Ca^{2+} . Because the mitochondrial Ca^{2+} efflux rates are reduced by 50 to 80% by CsA

(Fig. 2E), the steady-state $[Ca^{2+}]$ is also lower in the presence of CsA than in the control (Fig. 3A). Mitochondria only undergo net Ca^{2+} uptake at external Ca^{2+} levels exceeding the steady-state $[Ca^{2+}]$. Thus, this variable has been considered a threshold or an index of the affinity of the mitochondrial Ca^{2+} uptake system. Other researchers have demonstrated that physiological levels of Mg^{2+} and Na^+ play a major role in determining the steady-state Ca^{2+} levels in isolated mitochondria because Mg^{2+} inhibits MCU-mediated Ca^{2+} influx (16) and because Na^+ greatly stimulates mitochondrial Ca^{2+} efflux in some cell types (11). To prevent misleading interpretations about the steady-state $[Ca^{2+}]$, we must remember not only that Mg^{2+} and Na^+ ions are important regulators but also that a lack of control of MPT pore opening can bias results and comparisons.

There are theoretical reasons to set proper experimental conditions to maintain mitochondrial integrity during *in vitro* assays that are designed to evaluate function. Because Ca^{2+} -induced MPT causes dysfunction and loss of organelle integrity (4), any degree of MPT pore opening during the measurement of Ca^{2+} transport should be avoided. Direct evidence supporting this assertion has been provided here, and the correlations shown in Figs. 3E and F are rather valuable. Strong and significant correlations between the MRT and the steady-state $[Ca^{2+}]$ occur only under the condition of MPT inhibition by CsA.

In numerous studies, Ca^{2+} levels were titrated to determine the kinetics of mitochondrial Ca^{2+} uptake (2, 6, 24). A monoexponential dependence of flux rates on external Ca^{2+} levels was generally obtained, and the V_{max} and K_m values were estimated from this relationship in a *Michaelian* manner (6, 24, 37). In light of data in the literature and presented here, these monoexponential kinetics that lead to an asymptote (*i.e.*, V_{max}) may be related to the Ca^{2+} -induced mitochondrial dysfunction and energetic failure at higher $[Ca^{2+}]$ rather than to an intrinsic limit of the membrane potential-driven MCU activity. The evidence for this assertion is that the inhibition of MPT pore opening by CsA allows

measurements of mitochondrial Ca^{2+} transport at higher Ca^{2+} levels (**Figs. 2A** and **2B**), therefore changing the observed relationship between influx rates and external Ca^{2+} levels.

Diversity in mitochondrial Ca^{2+} handling across tissues. Due to interest in fundamental physiological functions, early studies attempted to investigate the tissue diversity of mitochondrial Ca^{2+} handling (6, 11, 12, 20, 21, 24, 45). As the implication of the first part of this study revealed the need for MPT inhibition, we sought to compare Ca^{2+} -handling variables between the sexes and tissues under suitable experimental conditions consisting of appropriate levels of free Ca^{2+} , Mg^{2+} and Na^+ and MPT inhibitors.

The variables assessed here show different degrees of tissue diversity. The respiratory rates (**Figs. 4A-C**) and Ca^{2+} efflux (**Figs. 5D-E**) exhibit more differences between tissues compared with the differences in mitochondrial Ca^{2+} influx, which has rates that are similar in the brain, heart and muscle mitochondria (Figs. 5A and 5B). Because of these tissue profiles, the combination of Ca^{2+} influx and efflux rates that describes the tendency (*i.e.*, Ca^{2+} influx: efflux ratio) for mitochondria to accumulate Ca^{2+} varies greatly across tissues. The mitochondria from the liver, the sole non-excitabile tissue evaluated here, exhibit the highest influx rate and the lowest efflux rate, resulting in an averaged influx: efflux ratio of nearly 500; in contrast, this ratio was less than 25 in the organelles from the other tissues, which were excitable. The physiological meaning of such tissue diversity for cellular and mitochondrial Ca^{2+} homeostasis deserves further investigation because this diversity might be related to the different roles of mitochondrial and cytosolic Ca^{2+} transients across cells/tissues. Using an electrophysiological technique to measure the MCU activity in the absence of MPT inhibitors and Mg^{2+} (an endogenous inhibitor of MCU activity whose potency is dependent on tissue mitochondria), Fieni et al. (17) showed that liver mitochondria presented intermediate MCU fluxes compared with the fluxes of mitochondria from skeletal muscle and heart; these two tissues exhibited the highest and the lowest Ca^{2+}

flux through MCU, respectively. Interestingly, the expression levels of MCU mRNA in a mouse heart are very similar to that in the liver, higher than that in brain and lower than that in skeletal muscle (13). Altogether, the studies collectively indicate that the MCU density in the IMM in and of itself may be of little significance to the MCU-mediated Ca^{2+} influx in *in situ* mitochondria because many intervening variables modify the activation (26, 34), the affinity and the energy that drive the mitochondrial Ca^{2+} influx through the MCU complex (14, 16, 36, 37). The membrane potential across the IMM and the free Mg^{2+} levels are known modulators of MCU-mediated Ca^{2+} influx (36, 37), and important discoveries on MCU molecular biology have now revealed regulatory roles for subunits of the MCU complex (26, 34), which may also exhibit varying expression levels in different tissues (13). Thus, mitochondrial Ca^{2+} influx constitutes a complex phenomenon involving biochemical regulation and cellular specificity.

The role of Ca^{2+} efflux pathways is critical to mitochondrial Ca^{2+} homeostasis (29, 43). The Ca^{2+} efflux from heart mitochondria has been considered to be highly dependent on the $\text{Na}^+/\text{Ca}^{2+}$ exchange via the NCLX transporter (29, 43), whereas the $\text{H}^+/\text{Ca}^{2+}$ exchanger would provide a minor or even null contribution to the Ca^{2+} efflux (35). Previous studies showed that the Na^+ -present Ca^{2+} efflux from heart mitochondria is several fold higher than the Na^+ -independent pathway (10, 22, 38, 46). It is critical to bear in mind that in most of the studies supporting this notion, the Ca^{2+} efflux was assayed in the absence of Mg^{2+} and succinate was used as an energizing substrate. Conversely, using an incubation medium containing 1 mM free Mg^{2+} and NAD-linked substrates, we found here that the Ca^{2+} efflux through the $\text{H}^+/\text{Ca}^{2+}$ exchanger in heart mitochondria is not negligible (**Fig. 5C**) and that Na^+ stimulates the mitochondrial Ca^{2+} efflux by only ~100% (**Fig. 5E**). Such apparent divergence between our findings and previous concepts led us to evaluate the heart mitochondrial Ca^{2+} efflux in the absence of Mg^{2+} and with succinate as an energizing

substrate. Under such experimental conditions (**Fig. 7**), we very closely reproduced the previous findings. Nonetheless, similarly to our data, evidence elsewhere shows significant Na^+ -independent Ca^{2+} efflux from heart mitochondria energized by succinate in the absence of Mg^{2+} that should not remain unnoticed (10, 20). In fact, our data show that the choice of exogenous substrates that energize heart mitochondria profoundly affects the rates of Ca^{2+} efflux from heart mitochondria, particularly through the $\text{Na}^+/\text{Ca}^{2+}$ exchanger pathway. However, the mechanisms underlying this interesting phenomenon are not clear.

Sex diversity in mitochondrial functions. Estrogens are able to modulate mitochondria biogenesis in some cells (7), and rat liver mitochondrial respiration differs by sex in rats (44); thus, it was tempting to investigate whether such sex dimorphism would occur in other tissues and whether this difference would also involve Ca^{2+} handling by mitochondria. Likewise, previous studies showed lower levels of PGC1 α and TFAM and lower activities of respiratory complexes III and IV in the whole hearts of female rats compared with those of male rats (8). Analyzing only left heart ventricles, Arieli et al (1) showed that the uptake of Ca^{2+} (assayed in the absence of Mg^{2+}) by isolated mitochondria from females was slower than that in males (1). Although we did not observe significant sex differences in the mitochondrial Ca^{2+} influx rates even in heart organelles (**Fig. 5A and B**), the variables that reflect the concentration threshold for net Ca^{2+} uptake (**Fig. 5G**) and the time required to internalize an external Ca^{2+} load (**Fig. 6B**) were higher in the female heart mitochondria than in male heart mitochondria. With the exception of sex differences in liver mitochondria respiratory rates under phosphorylation conditions (**Fig. 4B**), none of the remaining assayed variables in our Mg^{2+} -containing medium exhibited sex dimorphism in the present study.

In summary, we show here the methodological importance of controlling MPT pore opening during Ca^{2+} transport assays, and the lack of this control may bias measurements

of the mitochondrial Ca^{2+} efflux through Na^+ -independent and Na^+ -dependent pathways. Accounting for the implied importance of controlling MPT pore opening, we then observed substantial tissue specificities in the mitochondrial Ca^{2+} handling, particularly in the Ca^{2+} efflux pathways from mitochondria. In contrast, rat sex only affected respiration during the phosphorylation condition in liver mitochondria and two indexes of Ca^{2+} homeostasis in heart mitochondria.

Acknowledgments

We are grateful to Edilene S. Siqueira Santos and Roberto C. Stahl for their technical assistance.

Grants

Research funding was provided by FAPESP (#11/50400-0) and CNPq. T.R.F is currently supported by a postdoctoral FAPESP fellowship (#2011/51800-1). H.C. was supported by a graduate scholarship from CAPES.

Disclosures

All authors report that they have no conflict of interest regarding the content of this manuscript.

References

1. **Arieli Y, Gursahani H, Eaton MM, Hernandez LA, and Schaefer S.** Gender modulation of Ca(2+) uptake in cardiac mitochondria. *J Mol Cell Cardiol*37: 507-513, 2004.
2. **Bassani RA, Fagian MM, Bassani JW, and Vercesi AE.** Changes in calcium uptake rate by rat cardiac mitochondria during postnatal development. *J Mol Cell Cardiol*30: 2013-2023, 1998.
3. **Baughman JM, Perocchi F, Girgis HS, Plovanich M, Belcher-Timme CA, Sancak Y, Bao XR, Strittmatter L, Goldberger O, Bogorad RL, Koteliansky V, and Mootha VK.** Integrative genomics identifies MCU as an essential component of the mitochondrial calcium uniporter. *Nature* 476: 341-345, 2011.
4. **Bernardi P.** Mitochondrial transport of cations: channels, exchangers, and permeability transition. *Physiol Rev* 79: 1127-1155, 1999.
5. **Boyman L, Williams GS, Khananshvil D, Sekler I, and Lederer WJ.** NCLX: the mitochondrial sodium calcium exchanger. *J Mol Cell Cardiol*59: 205-213, 2013.
6. **Bragadin M, Pozzan T, and Azzone GF.** Kinetics of Ca²⁺ carrier in rat liver mitochondria. *Biochemistry* 18: 5972-5978, 1979.
7. **Chen JQ, Cammarata PR, Baines CP, and Yager JD.** Regulation of mitochondrial respiratory chain biogenesis by estrogens/estrogen receptors and physiological, pathological and pharmacological implications. *Biochim Biophys Acta* 1793: 1540-1570, 2009.
8. **Colom B, Oliver J, Roca P, and Garcia-Palmer FJ.** Caloric restriction and gender modulate cardiac muscle mitochondrial H₂O₂ production and oxidative damage. *Cardiovasc Res* 74: 456-465, 2007.
9. **Crompton M, Ellinger H, and Costi A.** Inhibition by cyclosporin A of a Ca²⁺-dependent pore in heart mitochondria activated by inorganic phosphate and oxidative stress. *Biochem J* 255: 357-360, 1988.
10. **Crompton M, Heid I, Baschera C, and Carafoli E.** The resolution of calcium fluxes in heart and liver mitochondria using the lanthanide series. *FEBS Lett* 104: 352-354, 1979.
11. **Crompton M, Moser R, Ludi H, and Carafoli E.** The interrelations between the transport of sodium and calcium in mitochondria of various mammalian tissues. *Eur J Biochem*82: 25-31, 1978.
12. **Crompton M SE, Salzmann M, Carafoli E.** A Kinetic study of the energy-linked influx of Ca²⁺ into heart mitochondria. *Eur J Biochem*69: 6, 1976.
13. **De Stefani D, Raffaello A, Teardo E, Szabo I, and Rizzuto R.** A forty-kilodalton protein of the inner membrane is the mitochondrial calcium uniporter. *Nature* 476: 336-340, 2011.
14. **De Stefani D, and Rizzuto R.** Molecular control of mitochondrial calcium uptake. *Biochem Biophys Res Commun*449: 373-376, 2014.
15. **Elrod JW, Wong R, Mishra S, Vagnozzi RJ, Sakthivel B, Goonasekera SA, Karch J, Gabel S, Farber J, Force T, Brown JH, Murphy E, and Molkentin JD.** Cyclophilin D controls mitochondrial pore-dependent Ca(2+) exchange, metabolic flexibility, and propensity for heart failure in mice. *J Clin Invest* 120: 3680-3687, 2010.
16. **Favaron M, and Bernardi P.** Tissue-specific modulation of the mitochondrial calcium uniporter by magnesium ions. *FEBS Lett* 183: 260-264, 1985.
17. **Fieni F, Lee SB, Jan YN, and Kirichok Y.** Activity of the mitochondrial calcium uniporter varies greatly between tissues. *Nat Commun*3: 1317, 2012.

18. **Figueira TR, Barros MH, Camargo AA, Castilho RF, Ferreira JC, Kowaltowski AJ, Sluse FE, Souza-Pinto NC, and Vercesi AE.** Mitochondria as a source of reactive oxygen and nitrogen species: from molecular mechanisms to human health. *Antioxid Redox Signal* 18: 2029-2074, 2013.
19. **Figueira TR, Caputo F, Machado CE, and Denadai BS.** Aerobic Fitness Level Typical of Elite Athletes is not Associated With Even Faster VO₂ Kinetics During Cycling Exercise. *J Sports Sci Med* 7: 132-138, 2008.
20. **Harris EJ.** Modulation of Ca²⁺ efflux from heart mitochondria. *Biochem J* 178: 673-680, 1979.
21. **Harris EJ.** The uptake and release of calcium by heart mitochondria. *Biochem J* 168: 447-456, 1977.
22. **Harris EJ, and Heffron JJ.** The stimulation of the release of Ca²⁺ from mitochondria by sodium ions and its inhibition. *Arch Biochem Biophys* 218: 531-539, 1982.
23. **Haworth RA, Hunter DR, and Berkoff HA.** Na⁺ releases Ca²⁺ from liver, kidney and lung mitochondria. *FEBS Lett* 110: 216-218, 1980.
24. **Jacobus WE, Tiozzo R, Lugli G, Lehninger AL, and Carafoli E.** Aspects of energy-linked calcium accumulation by rat heart mitochondria. *J Biol Chem* 250: 7863-7870, 1975.
25. **Justo R, Boada J, Frontera M, Oliver J, Bermudez J, and Gianotti M.** Gender dimorphism in rat liver mitochondrial oxidative metabolism and biogenesis. *Am J Physiol Cell Physiol* 289: C372-378, 2005.
26. **Kamer KJ, and Mootha VK.** MICU1 and MICU2 play nonredundant roles in the regulation of the mitochondrial calcium uniporter. *EMBO Rep* 15: 299-307, 2014.
27. **Kaplan RS, and Pedersen PL.** Characterization of phosphate efflux pathways in rat liver mitochondria. *Biochem J* 212: 279-288, 1983.
28. **Kirichok Y, Krapivinsky G, and Clapham DE.** The mitochondrial calcium uniporter is a highly selective ion channel. *Nature* 427: 360-364, 2004.
29. **Maack C, Cortassa S, Aon MA, Ganesan AN, Liu T, and O'Rourke B.** Elevated cytosolic Na⁺ decreases mitochondrial Ca²⁺ uptake during excitation-contraction coupling and impairs energetic adaptation in cardiac myocytes. *Circ Res* 99: 172-182, 2006.
30. **Nicholls DG, and Brand MD.** The nature of the calcium ion efflux induced in rat liver mitochondria by the oxidation of endogenous nicotinamide nucleotides. *Biochem J* 188: 113-118, 1980.
31. **Nicholls DG, and Crompton M.** Mitochondrial calcium transport. *FEBS Lett* 111: 261-268, 1980.
32. **Palty R, Silverman WF, Hershinkel M, Caporale T, Sensi SL, Parnis J, Nolte C, Fishman D, Shoshan-Barmatz V, Herrmann S, Khananshvil D, and Sekler I.** NCLX is an essential component of mitochondrial Na⁺/Ca²⁺ exchange. *Proc Natl Acad Sci U S A* 107: 436-441, 2010.
33. **Pan X, Liu J, Nguyen T, Liu C, Sun J, Teng Y, Fergusson MM, Rovira II, Allen M, Springer DA, Aponte AM, Gucek M, Balaban RS, Murphy E, and Finkel T.** The physiological role of mitochondrial calcium revealed by mice lacking the mitochondrial calcium uniporter. *Nat Cell Biol* 15: 1464-1472, 2013.
34. **Patron M, Checchetto V, Raffaello A, Teardo E, Vecellio Reane D, Mantoan M, Granatiero V, Szabo I, De Stefani D, and Rizzuto R.** MICU1 and MICU2 finely tune the mitochondrial Ca²⁺ uniporter by exerting opposite effects on MCU activity. *Mol Cell* 53: 726-737, 2014.

35. **Pizzo P, Drago I, Filadi R, and Pozzan T.** Mitochondrial Ca²⁺(+) homeostasis: mechanism, role, and tissue specificities. *Pflugers Arch* 464: 3-17, 2012.
36. **Pradhan RK, Qi F, Beard DA, and Dash RK.** Characterization of membrane potential dependency of mitochondrial Ca²⁺ uptake by an improved biophysical model of mitochondrial Ca²⁺ uniporter. *PLoS One* 5: e13278, 2010.
37. **Pradhan RK, Qi F, Beard DA, and Dash RK.** Characterization of Mg²⁺ inhibition of mitochondrial Ca²⁺ uptake by a mechanistic model of mitochondrial Ca²⁺ uniporter. *Biophys J* 101: 2071-2081, 2011.
38. **Rizzuto R, Bernardi P, Favaron M, and Azzone GF.** Pathways for Ca²⁺ efflux in heart and liver mitochondria. *Biochem J* 246: 271-277, 1987.
39. **Ronchi JA, Figueira TR, Ravagnani FG, Oliveira HC, Vercesi AE, and Castilho RF.** A spontaneous mutation in the nicotinamide nucleotide transhydrogenase gene of C57BL/6J mice results in mitochondrial redox abnormalities. *Free Radic Biol Med* 63: 446-456, 2013.
40. **Rosenthal RE, Hamud F, Fiskum G, Varghese PJ, and Sharpe S.** Cerebral ischemia and reperfusion: prevention of brain mitochondrial injury by lidoflazine. *J Cereb Blood Flow Metab* 7: 752-758, 1987.
41. **Saito A, and Castilho RF.** Inhibitory effects of adenine nucleotides on brain mitochondrial permeability transition. *Neurochem Res* 35: 1667-1674, 2010.
42. **Tahara EB, Navarete FD, and Kowaltowski AJ.** Tissue-, substrate-, and site-specific characteristics of mitochondrial reactive oxygen species generation. *Free Radic Biol Med* 46: 1283-1297, 2009.
43. **Takeuchi A, Kim B, and Matsuoka S.** The mitochondrial Na⁺-Ca²⁺ exchanger, NCLX, regulates automaticity of HL-1 cardiomyocytes. *Sci Rep* 3: 2766, 2013.
44. **Valle A, Guevara R, Garcia-Palmer FJ, Roca P, and Oliver J.** Sexual dimorphism in liver mitochondrial oxidative capacity is conserved under caloric restriction conditions. *Am J Physiol Cell Physiol* 293: C1302-1308, 2007.
45. **Vinogradov A, and Scarpa A.** The initial velocities of calcium uptake by rat liver mitochondria. *J Biol Chem* 248: 5527-5531, 1973.
46. **Wei AC, Liu T, Cortassa S, Winslow RL, and O'Rourke B.** Mitochondrial Ca²⁺ influx and efflux rates in guinea pig cardiac mitochondria: low and high affinity effects of cyclosporine A. *Biochim Biophys Acta* 1813: 1373-1381, 2011.
47. **Williams GS, Boyman L, Chikando AC, Khairallah RJ, and Lederer WJ.** Mitochondrial calcium uptake. *Proc Natl Acad Sci U S A* 110: 10479-10486, 2013.
48. **Wingrove DE, and Gunter TE.** Kinetics of mitochondrial calcium transport. I. Characteristics of the sodium-independent calcium efflux mechanism of liver mitochondria. *J Biol Chem* 261: 15159-15165, 1986.
49. **Zhu L, Yu Y, Chua BH, Ho YS, and Kuo TH.** Regulation of sodium-calcium exchange and mitochondrial energetics by Bcl-2 in the heart of transgenic mice. *J Mol Cell Cardio* 33: 2135-2144, 2001.
50. **Zimmerman Donald .W.** A Note on Interpretation of the Paired-Samples t Test *Journal of Educational and Behavioral Statistics*. Vol. 22, No. 3 (Autumn, 1997), pp. 349-360

4.CONCLUSÕES

Conclui-se que a prevenção da abertura do poro de TPM durante os ensaios de transporte de Ca^{2+} é de importância metodológica. Não impedi-lo pode acarretar em alterações dos valores das variáveis que descrevem o transporte de Ca^{2+} , especialmente promovendo a superestimativa das taxas de efluxo e do *steady-state* de Ca^{2+} mitocondrial.

Em relação aos dados relacionados com o dimorfismo sexual para as funções mitocondriais aqui avaliadas, pode-se verificar que os mesmos são tecido-específicas. Porém, o dimorfismo observado foi restrito apenas à:

- Respiração máxima estimulada por ADP em mitocôndrias isoladas de fígado de ratos macho e fêmea, sendo maior na fêmea;
- Concentração de Ca^{2+} no *steady-state* mais elevada nas mitocôndrias de coração de fêmea;
- MRT normalizado mais lento nas mitocôndrias de coração de fêmea.

5. REFERÊNCIAS

1. Lehninger, A.L., D. L. Nelson , M. M .Cox, *Princípios de Bioquímica de Lehninger*.5 ed ed. 2011, Porto Alegre: Artmed.
2. Lehninger, A.L., *The mitochondrion: molecular basis of structure and function*. WABenjamin,, 1964.
3. Liesa, M., M. Palacin, and A. Zorzano, *Mitochondrial dynamics in mammalian health and disease*. *Physiol Rev*, 2009. **89**(3): p. 799-845.
4. Altmann, R., *Die Elementarorganismen Und Ihre Beziehungen Zu Den Zellen*. .Veit & comp, 1890. **145**.
5. Mitchell, P., *Coupling of phosphorylation to electron and hydrogen transfer by a chemi-osmotic type of mechanism*. *Nature*, 1961. **v.191**: p. p.144-8.
6. Nicholls, D.G., S. J. Ferguson., *Proton Current and Respiratory Control*. Academic Press Inc, 2002. **v.3**: p. p.69-75.
7. De Pinto, V., S. Reina, et al., *Structure of the voltage dependent anion channel: state of the art*. *J Bioenerg Biomembr*, 2008. **v.40**: p. p.139-47.
8. Figueira, T.R., et al., *Mitochondria as a source of reactive oxygen and nitrogen species: from molecular mechanisms to human health*. *Antioxid Redox Signal*, 2013. **18**(16): p. 2029-74.
9. Laura D. Osellame, T.S.B., Michael R. Duchen,, *Cellular and molecular mechanisms of mitochondrial function*. *Best Practice & Research Clinical Endocrinology & Metabolism*, 2012. **26**: p. 711-726.
10. Nicholls, D.G., S. J. Ferguson., *Proton Current and Respiratory Control*. 2002.
11. Vercesi, A.E., J. , *Plant uncoupling mitochondrial proteins*. *Annu Rev Plant Biol*, 2006a. **v.57**: p. p.383-404.
12. Packer, L., *Size and shape transformations correlatedwith oxidative phosphorylation in mitochondria*. *J Cell Biol*, 1963. **v.18**: p. p.487-94.
13. Mannella, C.A., *The relevance of mitochondrial membrane topology to mitochondrial function*. *Biochim Biophys Acta*, 2006. **v.762**: p. p.140-7.
14. Osmundsen, H., J. Cervenkat, J. Bremert., *A role for 2,4-enoyl-CoA reductase in mitochondrial f-oxidation of polyunsaturated fatty acids: Effects of treatment with clofibrate on oxidation of polyunsaturated acylcarnitines by isolated rat liver mitochondria*. *Biochem. J.*, 1982. **v.208**: p. p.749-57.
15. Brady, L.J., C. L. Hoppel, P. S. Brady., *Hepatic mitochondrial inner-membrane properties, beta-oxidation and carnitine palmitoyltransferases A and B. Effects of genetic obesity and starvation*. *Biochem J.*, 1986. **v.15**: p. p.427–33.
16. Herrmann, J.M., J. Riemer., *The intermembrane space of mitochondria*. *Antioxid Redox Signal*, 2010. **v.13**: p. p.1341-58.
17. Mannella, C.A., et al., *Topology of the mitochondrial inner membrane: dynamics and bioenergetic implications*. *IUBMB Life*, 2001. **52**(3-5): p. 93-100.
18. Berridge, M.J., *Cardiac calcium signaling*. *Biochem Soc Trans*, 2003. **v.31**: p. p.930-3.

19. Gunter, T.E. and D.R. Pfeiffer, *Mechanisms by which mitochondria transport calcium*. Am J Physiol, 1990. **258**(5 Pt 1): p. C755-86.
20. Chance, B., *The energy - linked reaction of calcium with mitochondria*. J. Biol. Chem, 1965: p. 2729-2748.
21. De Luca HF, E.G., *Ca²⁺ uptake by rat kidney mitochondria*. Proc Natl Acad Sci USA 1961. **47**: p. 1744-1750.
22. Vasington FD, M.J., *Ca ion uptake by rat kidney mitochondria and its dependence on respiration and phosphorylation*. . J Biol Chem 1962, 1962. **237**: p. 2670-7.
23. Lehninger AL, R.C., Greenawalt JW. , *Respiration-dependent accumulation of inorganic phosphate and Ca ions by rat liver mitochondria*. Biochem Biophys Res Commun 1963. **10**: p. 444-8.
24. Rapizzi, E., Pinton, P., Szabadkai, G., Wieckowski, M. R., Vandecasteele, G., Baird, G., Tuft, R. A., Fogarty, K. E., and Rizzuto, R. , *Recombinant expression of the voltage-dependent anion channel enhances the transfer of Ca²⁺ microdomains to mitochondria*. J. Cell Biol., 2002. **159**: p. 613-624.
25. Madesh, M., and Hajno ́czyk, G., *VDAC-dependent permeabilization of the outer mitochondrial membrane by superoxide induces rapid and massive cytochrome c release*. J. Cell Biol., 2001. **155**: p. 1003-1015.
26. Wingrove, D.E. and T.E. Gunter, *Kinetics of mitochondrial calcium transport. I. Characteristics of the sodium-independent calcium efflux mechanism of liver mitochondria*. J Biol Chem, 1986. **261**(32): p. 15159-65.
27. Nicholls, D.G. and M. Crompton, *Mitochondrial calcium transport*. FEBS Lett, 1980. **111**(2): p. 261-8.
28. Ying WL, E.J., Clarke MJ, Sanadi DR., *Inhibition of mitochondrial calcium ion transport by an oxo-bridged dinuclear ruthenium ammine complex..* Biochemistry, 1991. **30**: p. 4949-52.
29. Vinogradov, A. and A. Scarpa, *The initial velocities of calcium uptake by rat liver mitochondria*. J Biol Chem, 1973. **248**(15): p. 5527-31.
30. Bragadin, M., T. Pozzan, and G.F. Azzone, *Kinetics of Ca²⁺ carrier in rat liver mitochondria*. Biochemistry, 1979. **18**(26): p. 5972-8.
31. M. A. GOLDSTONE, A.M.L.E., *Calcium uptake by two preparations of mitochondria from heart*. Biochim. Biophys. Acta, 1980. **251-265**(591).
32. De Stefani, D., et al., *A forty-kilodalton protein of the inner membrane is the mitochondrial calcium uniporter*. Nature, 2011. **476**(7360): p. 336-40.
33. J.M. Baughman, F.P., H.S. Girgis, M. Plovanich, C.A. Belcher-Timme, Y. Sancak, X.R. Bao, L. Strittmatter, O. Goldberger, R.L. Bogorad, V. Kotliansky, V.K. Mootha,, *Integrative genomics identifies MCU as an essential component of the mitochondrial calcium uniporter*. Nature, 2011. **476**: p. 341-345.
34. R. Rizzuto, D.D.S., A. Raffaello, C. Mammucari *Mitochondria as sensors and regulators of calcium signalling*. Nat. Rev. Mol. Cell. Biol. , 2012. **13**: p. 566-578.
35. A. Raffaello, D.D.S., D. Sabbadin, E. Teardo, G. Merli, A. Picard, V.Checchetto, S. Moro, I. Szabo, R. Rizzuto, , *The mitochondrial calcium*

- uniporter is a multimer that can include a dominant-negative pore-forming subunit.* EMBO J, 2013. **32**: p. 2362-2376.
36. F. Perocchi, V.M.G., H.S. Girgis, X.R. Bao, J.E. McCombs, A.E. Palmer, V.K.Mootha, , *MICU1 encodes a mitochondrial EF hand protein required for Ca(2+) uptake.* Nature, 2010. **467**: p. 291-296.
 37. I. Drago, D.D.S., R. Rizzuto, T. Pozzan, , *Mitochondrial Ca²⁺ uptake contributes to buffering cytoplasmic Ca²⁺ peaks in cardiomyocytes.* Proc. Natl. Acad. Sci. U.S.A., 2012. **109**: p. 12986-12991.
 38. M.R. Alam, L.N.G., W. Parichatikanond, L. Kuo, A.I. Bondarenko, R. Rost, M. Waldeck-Weiermair, R. Malli, W.F. Graier, , *Mitochondrial Ca²⁺ uptake 1 (MICU1) and mitochondrial Ca²⁺ uniporter (MCU) contribute to metabolism secretion coupling in clonal pancreatic beta-cells.* J. Biol. Chem., 2012. **287**(34445-34454).
 39. S. Marchi, L.L., S. Patergnani, A. Rimessi, S. Missiroli, M. Bonora, A. Bononi, F. Corra, C. Giorgi, E. De Marchi, F. Poletti, R. Gafa, G. Lanza, M. Negrini, R. Rizzuto, P. Pinton., *Downregulation of the mitochondrial calcium uniporter by cancer-related miR-25.* Curr. Biol. , 2013. **23**: p. 58-63.
 40. J. Qiu, Y.W.T., A.M. Hagenston, M.A. Martel, N. Kneisel, P.A. Skehel, D.J. Wyllie, H. Bading, G.E. Hardingham, , *Mitochondrial calcium uniporter Mcu controls excitotoxicity and is transcriptionally repressed by neuroprotective nuclear calcium signals.* Nat. Commun., 2013. **4**: p. 2034.
 41. Bick AG, C.S., Mootha VK. , *Evolutionary diversity of the mitochondrial calcium uniporter.* Science, 2012. **336**: p. 886.
 42. Baughman, J.M., et al., *Integrative genomics identifies MCU as an essential component of the mitochondrial calcium uniporter.* Nature, 2011. **476**(7360): p. 341-5.
 43. Raffaello, A., et al., *The mitochondrial calcium uniporter is a multimer that can include a dominant-negative pore-forming subunit.* EMBO J, 2013. **32**(17): p. 2362-76.
 44. De Stefani, D. and R. Rizzuto, *Molecular control of mitochondrial calcium uptake.* Biochem Biophys Res Commun, 2014. **449**(4): p. 373-6.
 45. Alam MR, G.L., Parichatikanond W, Kuo L, Bondarenko AI, Rost R, et al., *Mitochondrial Ca²⁺ uptake 1 (MICU1) and mitochondrial Ca²⁺ uniporter (MCU) contribute to metabolism–secretion coupling in clonal pancreatic beta-cells.* J Biol Chem, 2012. **287**: p. 34445–54.
 46. Mallilankaraman K, D.P., Cardenas C, Chandramoorthy HC, Muller M, Miller R, et al. . *MICU1 is an essential gatekeeper for MCU-mediated mitochondrial Ca²⁺ uptake that regulates cell survival.* Cell, 2012. **151**: p. 630-44.
 47. Foskett JK, M.M., *Regulation of mitochondrial Ca²⁺ uniporter by MICU1 and MICU2.* Biochem Biophys Res Commun 2014. **449**: p. 377-83.
 48. Csordas G, G.T., Seifert EL, Kamer KJ, Sancak Y, Perocchi F, et al., *MICU1 controls both the threshold and cooperative activation of the mitochondrial Ca²⁺ uniporter.* Cell Metab, 2013. **17**: p. 976-87.

49. de la Fuente S, M.-I.J., Fonteriz RI, Montero M, Alvarez J. , *Dynamics of mitochondrial Ca²⁺ uptake in MICU1-knockdown cells*. Biochem J, 2014. **458**: p. 33-40.
50. Kamer, K.J. and V.K. Mootha, *MICU1 and MICU2 play nonredundant roles in the regulation of the mitochondrial calcium uniporter*. EMBO Rep, 2014. **15**(3): p. 299-307.
51. Patron M, C.V., Raffaello A, Teardo E, Vecellio Reane D, Mantoan M, et al. , *MICU1 and MICU2 finely tune the mitochondrial Ca²⁺ uniporter by exerting opposite effects on MCU activity*. Mol Cell, 2014. **53**: p. 726-37.
52. Plovanich M, B.R., Sancak Y, Kamer KJ, Strittmatter L, Li AA, et al. , *MICU2, a paralog of MICU1, resides within the mitochondrial uniporter complex to regulate calcium handling*. . PLoS One, 2013. **8**: p. e55785.
53. Mallilankaraman K, C.C., Doonan PJ, Chandramoorthy HC, Irrinki KM, Golenar T, et al. , *MCUR1 is an essential component of mitochondrial Ca²⁺ uptake that regulates cellular metabolism*. Nat Cell Biol, 2012. **15**: p. 123.
54. Sancak Y, M.A., Kitami T, Kovacs-Bogdan E, Kamer KJ, Udeshi ND, et al. and *EMRE is an essential component of the mitochondrial calcium uniporter complex*. Science, 2013. **342**: p. 1379-82.
55. Hoffman NE, C.H., Shamugapriya S, Zhang X, Rajan S, Mallilankaraman K, et al. , *MICU1 motifs define mitochondrial calcium uniporter binding and activity*. . Cell Rep, 2013. **5**: p. 1576-88.
56. Sancak, Y., et al., *EMRE is an essential component of the mitochondrial calcium uniporter complex*. Science, 2013. **342**(6164): p. 1379-82.
57. Huang, G., A.E. Vercesi, and R. Docampo, *Essential regulation of cell bioenergetics in Trypanosoma brucei by the mitochondrial calcium uniporter*. Nat Commun, 2013. **4**: p. 2865.
58. Crompton, M., et al., *The interrelations between the transport of sodium and calcium in mitochondria of various mammalian tissues*. Eur J Biochem, 1978. **82**(1): p. 25-31.
59. Pozzan T, A.G., *The coupling of electrical ion fluxes in rat liver mitochondria*. FEBS Lett, 1976. **72**: p. 62-66.
60. Pozzan T, B.M., Azzone GF *Disequilibrium between steady-state Ca²⁺ accumulation ratio and membrane potential in mitochondria. Pathway and role of Ca²⁺ efflux*. Biochemistry, 1977. **16**: p. 5618–5625.
61. Carafoli, E., *The release of calcium from heart mitochondria by sodium*. . J Mol Cell Cardiol, 1974. **6**: p. 361-71.
62. Crompton M, K.M., Carafoli E. , *The calcium-induced and sodium-induced effluxes of calcium from heart mitochondria. Evidence for a sodium-calcium carrier*. Eur J Biochem, 1977. **79**: p. 549-58.
63. Graier WF, T.M., Malli R. , *Mitochondrial Ca²⁺, the secret behind the function of uncoupling proteins 2 and 3?* . Cell Calcium, 2008. **44**: p. 36-50.
64. Lombardi A, G.P., Moreno M, de Lange P, Silvestri E, Lanni A, et al. , *Interrelated influence of superoxides and free fatty acids over mitochondrial uncoupling in skeletal muscle*. Biochim Biophys Acta, 2008. **1777**: p. 826-33.

65. Poburko D, S.-D.J., Demaurex N. , *Dynamic regulation of the mitochondrial proton gradient during cytosolic calcium elevations*. J Biol Chem, 2011. **286**: p. 11672–84.
66. Andrews ZB, D.S., Horvath TL. , *Mitochondrial uncoupling proteins in the CNS: in support of function and survival*. . Nat Rev Neurosci 2005. **6**: p. 829-40.
67. Haworth, R.A., D.R. Hunter, and H.A. Berkoff, *Na⁺ releases Ca²⁺ from liver, kidney and lung mitochondria*. FEBS Lett, 1980. **110**(2): p. 216-8.
68. Cai, X., *Molecular cloning of a sixth member of the K⁺-dependent Na⁺/Ca²⁺ exchanger gene family, NCKX6*. J Biol Chem, 2003. **279**: p. 5867–76.
69. Palty R, O.E., Hershinkel M, Volokita M, Elgazar V, Beharier O, et al. , *Lithium– calcium exchange is mediated by a distinct potassium-independent sodium–calcium exchanger*. J Biol Chem, 2004. **279**: p. 25234–40.
70. Anna Raffaello, D.D.S., Rosario Rizzuto, *The mitochondrial Ca²⁺ uniporter*. Cell Calcium, 2012. **52**: p. 16-21.
71. Hunter, D.R., R. A. Haworth, J. H. Southard. , *Relationship between configuration, function, and permeability in calcium-treated mitochondria*. J Biol Chem, 1976. **v.251**: p. p.5069-77.
72. Hunter, D.R., R. A. Haworth., *The Ca²⁺-induced mem-brane transition in mitochondria.I.The protective mechanisms*. Arch.Biochem. Biophys, 1979 a.. **v.195**: p. p.453-459.
73. Vercesi, A.E., A. J. Kowaltowski, et al. , *The role of reactive oxygen species in mitochondrial permeability transition*. Biosci Rep, 1997. **v.17**: p. p.43-52.
74. Kowaltowski, A.J., R. F. Castilho, A. E. Vercesi., *Mitochondrial permeability transition and oxidative stress*. FEBS Lett,, 2001 **v.495**: p. p.12-5.
75. Zoratti, M., I. Szabo. , *The mitochondrial permeability transition*. . Biochim Biophys Acta, 1995. **v.1241**: p. p.139-176.
76. Crompton, M., *The mitochondrial permeability transition pore and its role in cell death*. Biochem J, 1999. **v.341**: p. p.233-249.
77. Gunter, T.E., D. I. Yule, et al. , *Calcium and mitochondria*. FEBS Lett,, 2004. **v.567**: p. p.96-102.
78. Vercesi, A.E., A. J. Kowaltowski, et al. . *Mitochondrial Ca²⁺ transport, permeability transition and oxidative stress in cell death: implications in cardiotoxicity, neurodegeneration and dyslipidemias*. Front Biosci, , 2006b. **v.11**: p. p.2554-64.
79. Bernardi, P., *The mitochondrial permeability transition pore: a mystery solved?* Front Physiol,, 2013. **v.4**: p. p.95.
80. Le Quoc, K. and D. Le Quoc, *Involvement of the ADP/ATP carrier in calcium-induced perturbations of the mitochondrial inner membrane permeability: importance of the orientation of the nucleotide binding site*. Arch Biochem Biophys, 1988. **265**(2): p. 249-57.
81. Tsujimoto, Y. and S. Shimizu, *Role of the mitochondrial membrane permeability transition in cell death*. Apoptosis, 2007. **12**(5Role of the mitochondrial membrane permeability transition in cell death): p. 835-40.

82. Fagian, M.M., et al., *Membrane protein thiol cross-linking associated with the permeabilization of the inner mitochondrial membrane by Ca²⁺ plus prooxidants*. J Biol Chem, 1990. **265**(32): p. 19955-60.
83. Castilho, R.F., A.J. Kowaltowski, and A.E. Vercesi, *The irreversibility of inner mitochondrial membrane permeabilization by Ca²⁺ plus prooxidants is determined by the extent of membrane protein thiol cross-linking*. J Bioenerg Biomembr, 1996. **28**(6): p. 523-9.
84. Borel JF, K.Z., *The discovery and development of cyclosporine (Sandimmune)*. Transplant Proc, 1991. **23**: p. 1867–1874.
85. Handschumacher RE, H.M., Rice J, Drugge RJ, Speicher DW, *Cyclophilin: a specific cytosolic binding protein for cyclosporin A*. Science, 1984. **226**: p. 544-547.
86. Fournier N, D.G., Crevat A, *Action of cyclosporine on mitochondrial calcium fluxes*. . J Bioenerg Biomembr, 1987. **19**: p. 297-303.
87. Al Nasser I, C.M., *The reversible Ca²⁺-induced permeabilization of rat liver mitochondria*. Biochem J, 1986b. **239**: p. 19-29.
88. Crompton M, C.A., Hayat L, *Evidence for the presence of a reversible Ca²⁺-dependent pore activated by oxidative stress in heart mitochondria*. . Biochem J 1987. **245**: p. 915-918.
89. Crompton, M., H. Ellinger, and A. Costi, *Inhibition by cyclosporin A of a Ca²⁺-dependent pore in heart mitochondria activated by inorganic phosphate and oxidative stress*. Biochem J, 1988. **255**(1): p. 357-60.
90. Halestrap AP, D.A., *Inhibition of Ca²⁺(+)-induced large-amplitude swelling of liver and heart mitochondria by cyclosporin is probably caused by the inhibitor binding to mitochondrial-matrix peptidyl-prolyl cis-trans isomerase and preventing it interacting with the adenine nucleotide translocase*. Biochem J, 1990. **268**: p. 153-160.
91. Fischer G, W.-L.B., Lang K, Kiefhaber T, Schmid FX, *Cyclophilin and peptidyl-prolyl cis-trans isomerase are probably identical proteins*. . Nature, 1989. **337**: p. 476-478.
92. Tropschug M, N.D., Hartl FU, Kohler H, Pfanner N, Wachter E et al. , *Cyclosporin A-binding protein (cyclophilin) of Neurospora crassa. One gene codes for both the cytosolic and mitochondrial forms*. . J Biol Chem 1988. **263**: p. 14433-14440.
93. Saito, A. and R.F. Castilho, *Inhibitory effects of adenine nucleotides on brain mitochondrial permeability transition*. Neurochem Res. **35**(11): p. 1667-74.

6. ANEXO



CEUA/Unicamp

Comissão de Ética no Uso de Animais CEUA/Unicamp

CERTIFICADO

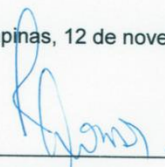
Certificamos que o projeto "Diferenças nas funções mitocondriais respiratórias e de transporte de Ca²⁺ entre machos e fêmeas" (protocolo nº 2897-1), sob a responsabilidade de Prof. Dr. Roger Frigério Castilho / Hanan Chweih, está de acordo com os Princípios Éticos na Experimentação Animal adotados pela Sociedade Brasileira de Ciência em Animais de Laboratório (SBCAL) e com a legislação vigente, LEI Nº 11.794, DE 8 DE OUTUBRO DE 2008, que estabelece procedimentos para o uso científico de animais, e o DECRETO Nº 6.899, DE 15 DE JULHO DE 2009.

O projeto foi aprovado pela Comissão de Ética no Uso de Animais da Universidade Estadual de Campinas - CEUA/UNICAMP - em 12 de novembro de 2012.

Campinas, 12 de novembro de 2012.



Prof. Dra. Ana Maria A. Guaraldo
Presidente



Fátima Alonso
Secretária Executiva

CEUA/UNICAMP
Caixa Postal 6109
13083-970 Campinas, SP – Brasil

Telefone: (19) 3521-6359
E-mail: comisib@unicamp.br
<http://www.ib.unicamp.br/ceea/>